MS-No.: egusphere-2024-2495

Title: Urban Area Observing System (UAOS) Simulation Experiment Using DQ-1 Total Column

Concentration Observations

Authors: Jinchun Yi, Yiyang Huang, Zhipeng Pei, Ge Han

Item-by-item reply to Anonymous Referee

July 23, 2025

Dear Christoph Gerbig and Reviewers,

We sincerely thank you and the reviewers for your constructive and thoughtful feedback on our manuscript. We have revised the manuscript accordingly and believe the revised version has improved in both clarity and scientific rigor. Please find below a detailed, point-by-point response to each reviewer comment.

- 1. The reviewers' comments are shown in black.
- 2. Our responses are also in blue, following each comment.
- 3. Descriptions of changes made to figures and tables are formatted in bold black text for clarity.

All modifications made to the manuscript are clearly marked in the revised version.

We greatly appreciate the reviewers' careful assessment and your editorial support. We hope the revised manuscript now meets the standards for publication.

Sincerely,

Jinchun Yi

On behalf of all co-authors

Wuhan University

Email: jinchun.yi@whu.edu.cn

Reply to Referee #1

Dear reviewer:

Thank you very much for reviewing our manuscript and providing valuable feedback. We sincerely appreciate your patience and detailed comments. Under your guidance, we have carefully addressed each of your comments and made corresponding revisions and additions. All your words are in black and our item-to-item responses are in blue. We have included our revisions for some comments directly for your convenience.

General comments:

The manuscript uses innovative active remote sensing CO2 data from the actual Chinese DQ-1 lidar satellite mission and shows the potential of the XCO2 IPDA lidar onboard DQ-1 to assess anthropogenic CO2 fluxes from megacities. The WRF-STILT model is used to assess atmospheric transport, and the ODIAC inventory provides emission estimates which are scaled to the observations using a regional inverse modelling approach. The authors additionally present a case study attempting at separating natural and anthropogenic CO2 emissions around Beijing, and investigate uncertainties due to measurement (XCO2) and model errors (wind speed and direction).

The data treatment and modelling approach is appropriate, but I am missing more details on how the background CO2 level is determined in the lidar measurements, which, in my experience, is a crucial issue. All major points are well presented, yet some statements, particularly those concerning the natural emissions, are based on the examination of very few cases, and thus need to be reformulated more cautiously. It would be helpful to include more megacity overpasses to consolidate the statements. Some figures have to be improved. The basic approach, the selection of two cities and the design of several figures is adopted from Ye et al (JGR-A 2020), so they should be more amply cited. The manuscript covers an important topic addressed with novel instrumentation and is a good match to ACP (or AMT). I therefore recommend accepting the manuscript, but only after my recommendations and comments have been addressed.

ANSWER: Thank you for your positive comments. We really appreciate your encouragement and support. To facilitate the readers' understanding of this study, we have carefully revised the whole manuscript according to your comments.

Mandatory changes:

1.Section 2.3.3 Background XCO2: own experience tells me that determining the background XCO2 level is the most critical part of data treatment. Please be more precise in the description of your DWT approach. Use the example of Fig 6b where I find the background gradient so strong that its determination must be particularly challenging. Add one or more plots to illustrate how the DWT works. Did you test other thresholds (line 247)? Why did you select mean + 0.5 sigma(XCO2) as threshold?

ANSWER: To derive ffXCO2, which represents the enhancement of XCO2 attributed to fossil fuel emissions, we need to subtract the background XCO2 from the observational data obtained by DQ-1(Ye et al., 2020). In the study by Ye et al. (2020), XCO2 is decomposed into two components:

 $XCO2_{trend}$ and $XCO2_{local}$. Here, $XCO2_{trend}$ represents the non-local trend, while the standard deviation σ_{local} of $XCO2_{local}$ indicates variations at the local scale. We filtered the XCO2 samples with $XCO2 < XCO2_{trend} + 0.5\sigma_{local}$ (the choice of $0.5\sigma_{local}$ as the threshold is mentioned here, and we conducted experiments with different thresholds. Given the similarity of our study area to that of Ye et al. (2022), we adopted her selected threshold for our experiments.) These filtered data are designated as "background samples" (represented by blue triangles in Figures 3, 5, 7, and S9) due to their lower spatial variability at the local scale compared to samples affected by urban ffCO2 emissions. We then performed linear regression based on the "background samples" to recalculate the linear regression line, referred to as the "background line." This "background line" method accounts for spatial trends in the background data. Unlike Ye et al. (2022), we utilized the low-frequency (approximate) coefficients obtained from DWT to characterize

The Discrete Wavelet Transform (DWT) is an approximate wavelet transformation method that decomposes a signal into approximation coefficients and detail coefficients at different scales. DWT employs discrete wavelet functions and discrete time scales, achieving signal decomposition through filtering and downsampling operations(Alessio et al., 2016). Typically, DWT decomposes a signal into a set of high-frequency and low-frequency sub-signals. Through successive decomposition, the discrete wavelet transform divides the data into different frequency bands. These frequency bands are generated by a series of wavelet and scaling functions, enabling the capture of both detailed and trend information within the data(Lang et al., 1995).

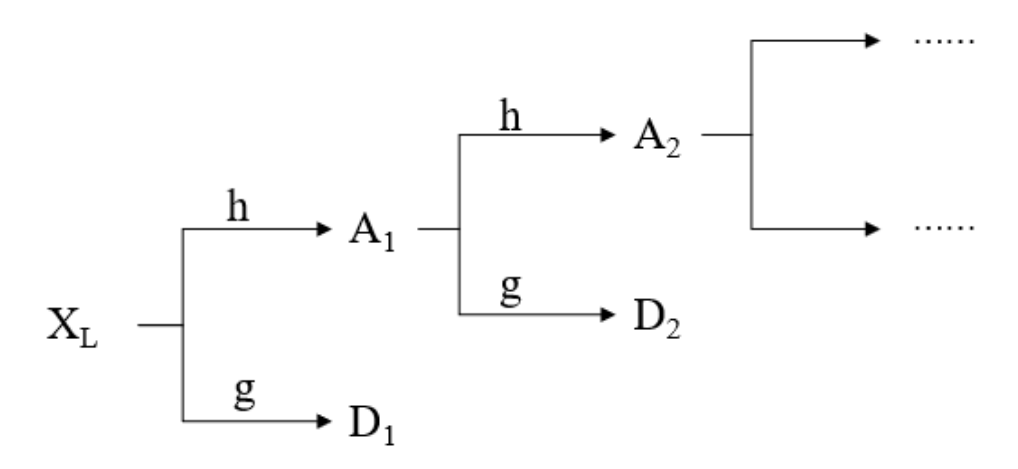


Figure S1. Schematic diagram of the principle of discrete wavelet transform

Figure S1 illustrates the working principle of the Discrete Wavelet Transform (DWT). For a signal XL of length L (representing the single-track DQ-1 XCO2 pseudo-data in this study), the wavelet transform (equivalent to a bandpass filter) decomposes it into high-pass coefficients D1 and approximation coefficients A1 (where the detail component D1 corresponds to filtering with a high-pass filter, and the approximation component A1 corresponds to filtering with a low-pass filter). The approximation coefficients are then further decomposed into relatively high-pass coefficients D2 and approximation coefficients A2, and this process continues iteratively. Figure S1 displays only two levels of wavelet decomposition. The equation for the first-level decomposition of DWT is as follows:

$$A_1(L) = \sum_k X_L(k) * h(k - L)$$

$$D_1(L) = \sum_k X_L(k) * g(k - L)$$
2

Where $A_1(L)$ represents the low-frequency (approximation) coefficients, and $D_1(L)$ denotes the high-frequency (detail) coefficients. h(k) and g(k) are the coefficients of the low-pass and high-pass wavelet filters, respectively. $X_L(k)$ is the initial input signal, and the input signal for the n-th level wavelet transform is A_{n-1} . We appreciate your inquiry regarding the background gradient in Figure 6b (now Figure 5b in the revised version) of the manuscript. Next, we will illustrate how to determine the background line using DWT and linear regression, using the track of DQ-1 passing over Beijing on December 1, 2022, as an example.

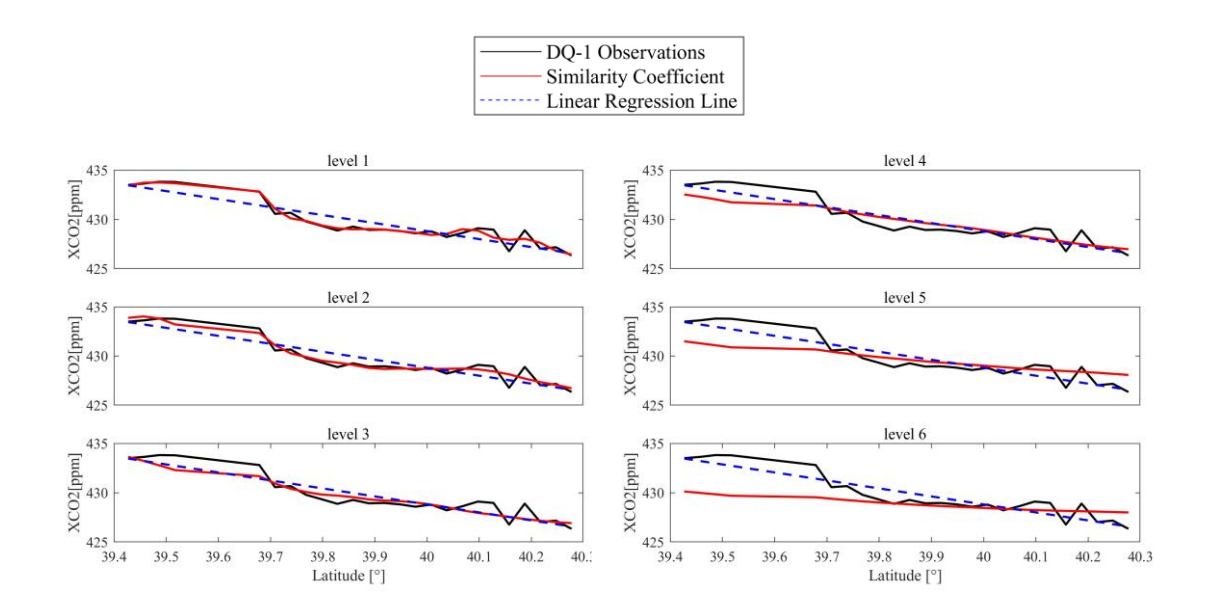


Figure S2. Level 1-6 wavelet transform applied to $XCO2_{trend}$ (red line in figure) derived from DQ-1 orbital pseudo-data (black line in figure) and $XCO2_{trend}$ derived from linear regression (blue dashed line in figure) for the DQ-1 orbital pseudo-data (black line in figure) transiting Beijing on 01 December 2022

Figure S2 displays the extracted $XCO2_{trend}$ from the 1st to the 6th levels of wavelet decomposition (shown as the red lines). The blue dashed lines in S2 represent the $XCO2_{trend}$ obtained using the linear regression method from the background line extraction approach of Ye et al. (2022). As the number of wavelet decomposition levels increases, the extracted $XCO2_{trend}$ becomes smoother and more horizontal, with decreasing gradient changes with latitude. Therefore, selecting an appropriate decomposition level based on different tracks is essential. It can be observed that the $XCO2_{trend}$ derived from the first and second levels of wavelet decomposition closely follows the trend of the pseudo-data along the track, failing to adequately filter out high-frequency information. In contrast, the $XCO2_{trend}$ from the third and fourth levels aligns more closely with the background line derived from linear regression, while the results from the fifth and sixth levels gradually approach horizontal, which does not conform to the desired background line that incorporates latitude gradients.

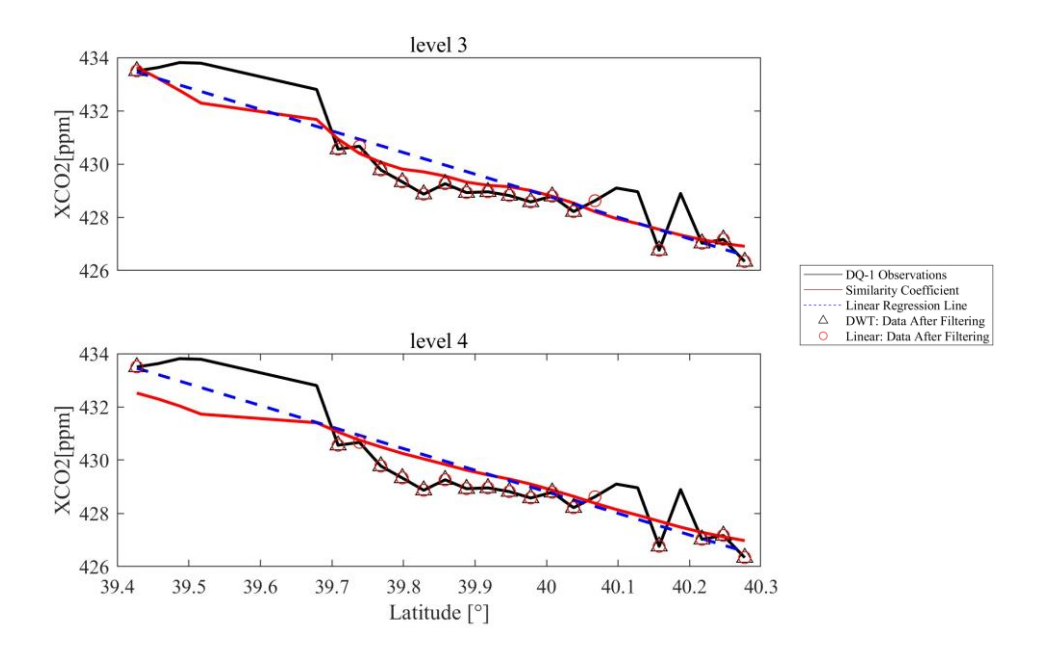


Figure S3. Pseudo-data points involved in the computation of the background line (black hollow triangles in the figure) screened using the third- and fourth-level wavelet transforms, respectively, and background points (red hollow circles) screened using linear regression. The black, red line and blue dashed line are the same as defined in Figure S2.

Figure S3 illustrates the $XCO2_{trend}$ extracted using the third and fourth levels of wavelet decomposition (red lines) from the DQ-1 pseudo-data passing over Beijing on December 1, 2022, along with the data points used for background line calculations (black hollow triangles). Additionally, it includes the $XCO2_{trend}$ extracted using the method of Ye et al. (2022) (blue dashed lines) and the corresponding data points for background line calculations (red hollow circles). In this scenario, the data points used for calculating the background line from the third and fourth wavelet levels are identical. However, the linear regression method filters out two more data points (39.7389° N and 40.0677° N) compared to the DWT approach.

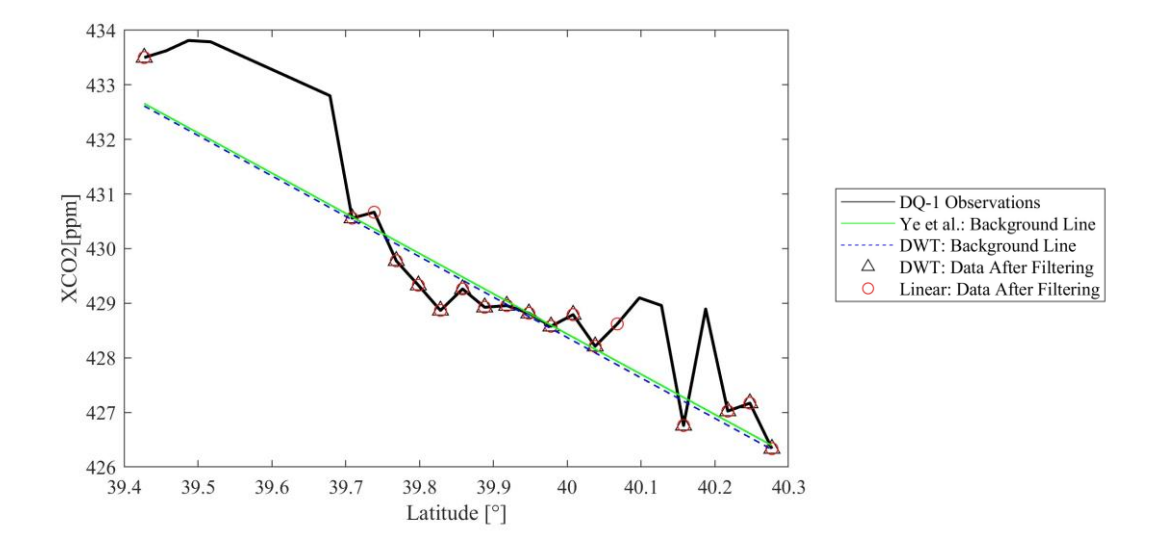


Figure S4. Background line derived using DWT (blue dashed line) and background line derived from linear regression (green line). The black line represents pseudo-observations from DQ-1, the black hollow triangles are background points filtered using DWT, and the red hollow circles are background points filtered by linear regression.

Figure S4 presents the background lines derived from the DQ-1 pseudo-data passing over Beijing on December 1, 2022, using the DWT method (blue dashed line) and the method from Ye et al. (2022) (green line). It is evident that although there is a difference of two data points in the selection of background data for calculations using these two methods, the extracted background lines are essentially indistinguishable.

2. Figure 3: It is unclear where the CO2 maxima in panels a and b come from, given that panels c and d show complex wind situations. Please add the column averaged footprint figures (like fig 2c) to clarify this. Could the maximum at 24.2 N in panel a come from another source in the southeast? The easterly winds suggest this. Please explain. Panels c and d are too small to see the colored DQ-1 XCO2 data, only the orbits are visible. Explain in the caption the blue triangles.

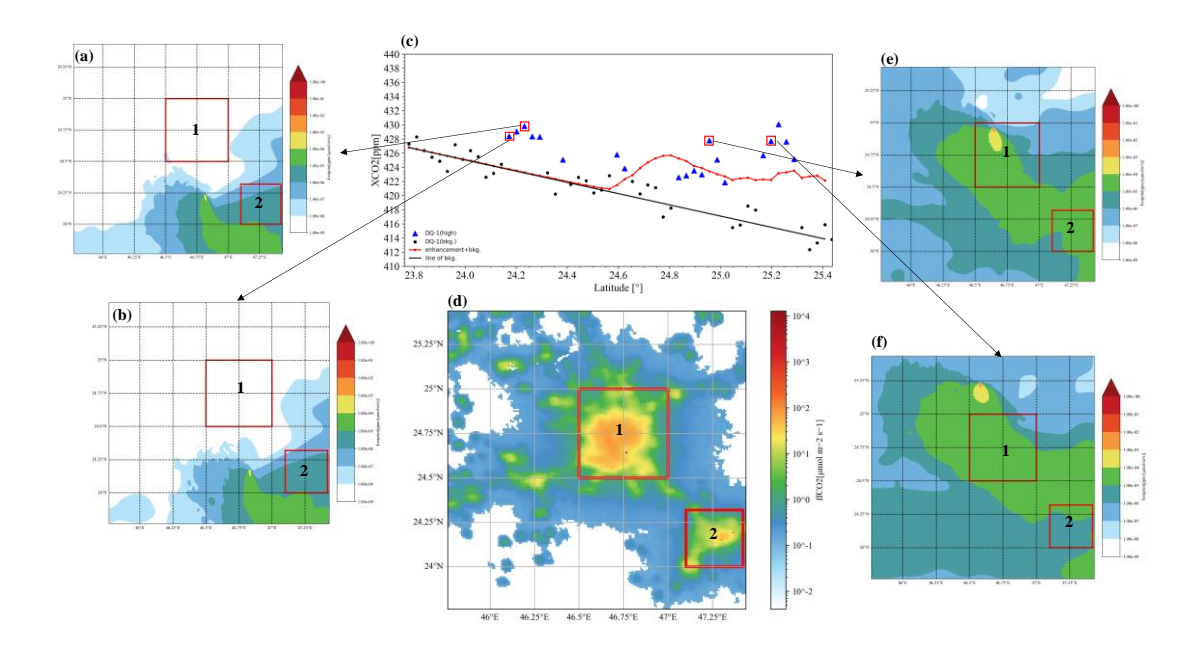


Figure S5. Shows the XSTILT (a, b, e, f) at the location of the partially apparent XCO2 enhancement in the orbit in Fig. 3a of the manuscript. Panel c is Figure 3a from the manuscript and panel d represents the fossil fuel emission inventory now of orbital transit. The main emission sources in the urban area are boxed in red.

ANSWER: Thank you very much for your insightful questions and suggestions regarding Figure 3 in the manuscript. Figure S5 illustrates the enhanced XSTILT data from the orbital data passing over Riyadh on March 2, 2023 (Figure S5c corresponds to Figure 3a in the manuscript), with panels S5a, b, e, and f showing specific enhancements. Panel S5d displays the ODIAC fossil fuel emissions inventory for this track, with two red boxes indicating the locations of major emissions sources (which correspond to the same latitude and longitude ranges as the red boxes in panels S5a, b, e, and f). Panels a and b show that the DQ-1 observational data recorded significant enhancements in XCO2, which were not captured by the simulation results. You mentioned in your suggestions whether the peak at 24.2°N in Figure 3a might originate from another source in the southeast. The easterly winds seem to support this possibility. In our study area, the southeastern source comes from red box 2, and the footprint observed in panels a and b at this location is less than 1e-05. Therefore, it can be concluded that the source in region 2 has a minimal impact on the enhancement of XCO2. The observed XCO2 enhancement from DQ-1 may be influenced by sources located outside the southeastern boundary of the study area. In panels e and f, it can be seen that the observed XCO2 enhancements at these two locations are consistent with the simulated XCO2 enhancements, primarily influenced by source 1 (red box 1).

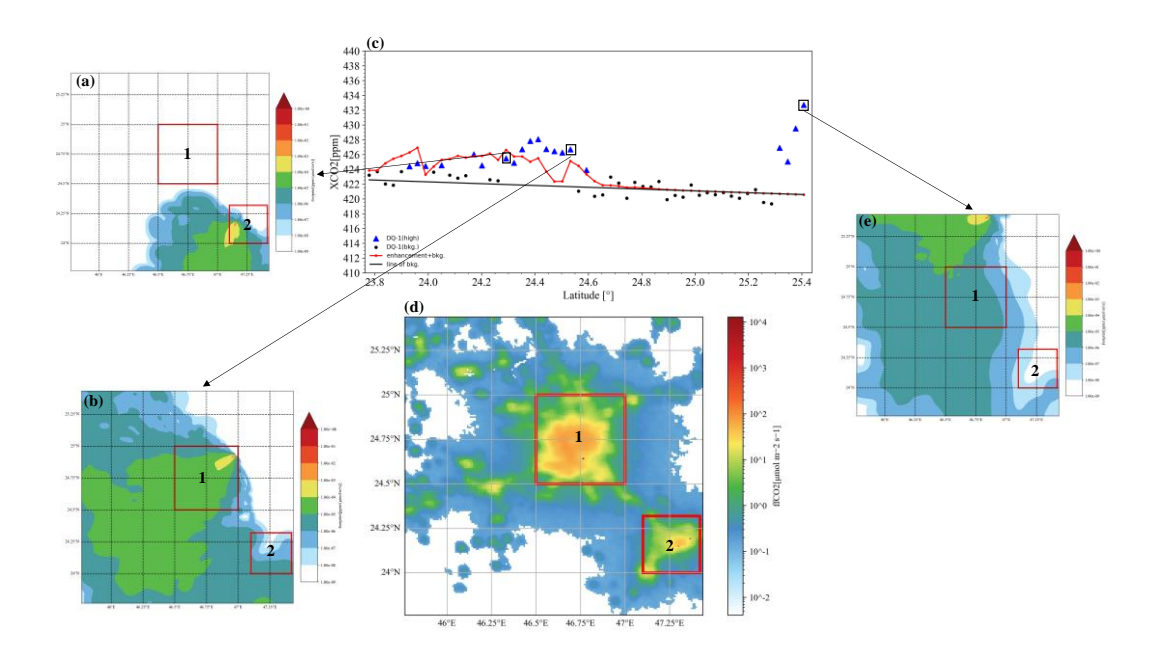


Figure S6. Like Fig. S5, the XSTILT for the case of Fig. 3b in the manuscript is shown (a, b, e).

Panels a and b illustrate the XCO2 enhancements simulated from sources 1 and 2, with the larger footprint locations showing a high degree of overlap with the sources (indicated by the red boxes). The enhancement observed at the 25.3-25.4° position may be influenced by sources located north of the study area.

In your second review comment, you noted that panels c and d are too small to view the colored DQ-1 XCO2 data, only showing the track. The original DQ-1 track data was too dense to clearly display the colored data, so we replaced it with pseudo-data tracks. We have also added an explanation in the figure caption regarding the blue triangles, which represent satellite-observed XCO2 data not used in the background line calculations (as we consider these to reflect the impacts of fossil fuel emission enhancements).

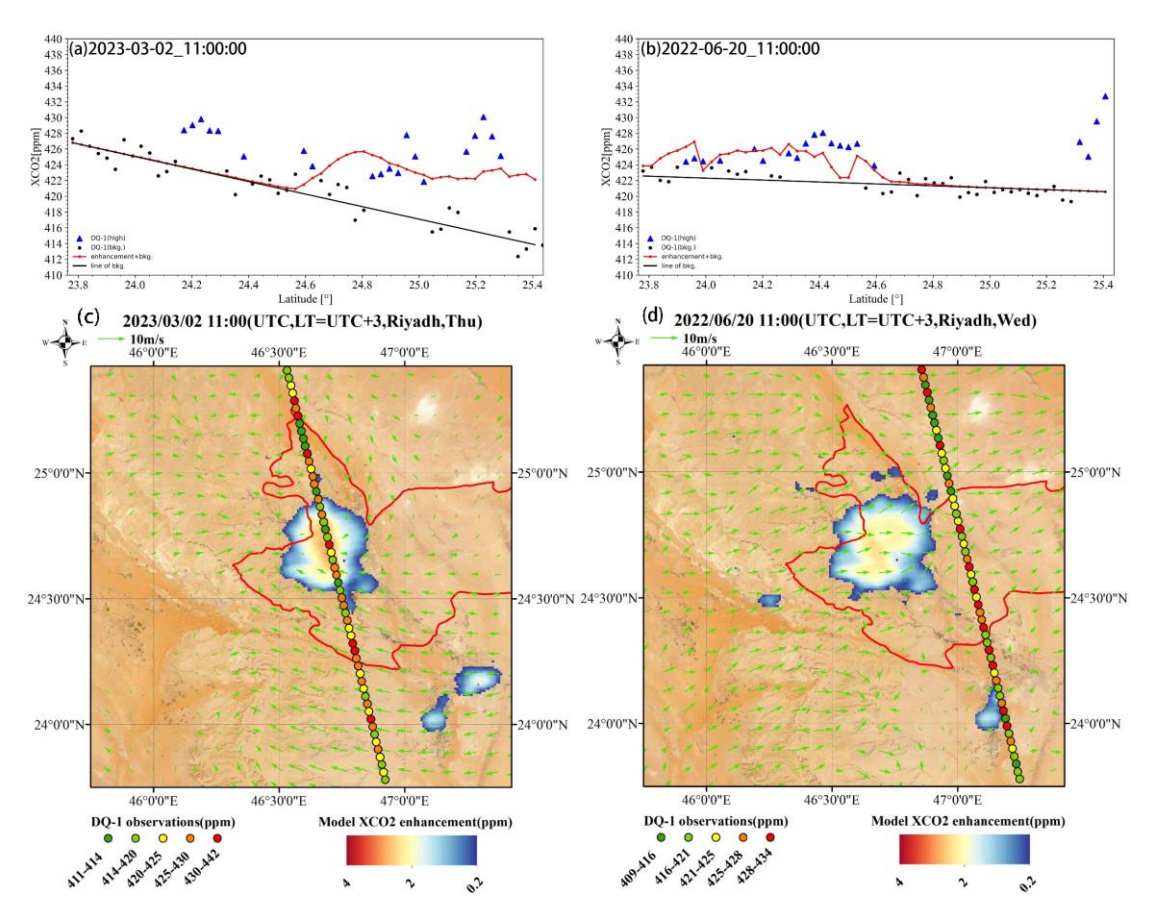


Figure 3. Comparison of the simulated and observed ffXCO2 enhancements from DQ-1 data over Riyadh on March 02, 2023 and June 20, 2022 around 11:00 UTC. Figures (a) and (b) show the DQ-1 XCO2 (black dots and blue triangles) and the simulated XCO2 (red solid line, sum of simulated ffXCO2 and background concentrations) along the two orbits, averaged over 1 s. The black dots represent the background concentrations involved in deriving the background. The black dots represent the data involved in the derivation of the background concentration (black solid line), which are linearly regressed against latitude after a discrete wavelet transform. Figures (c) and (d) show the simulated ffXCO2 and the observed ffXCO2 obtained from the DQ-1 data. background XCO2 concentrations have been subtracted. Vectors represent 10 m wind speeds (average wind speed simulated by WRF) and reference vectors represent 10 m/s wind speeds.

3. Figure 4: Please add the column averaged footprint figures (like fig 2c) to clarify the complex wind situations. The wind arrows are to small. All color bars seem wrong: the enhancements in the left line plots are much higher than in the right color plots.

ANSWER: Thank you very much for your suggestions regarding the revisions to Figure 4 (now Figure S9 in the revised version) in the manuscript. You requested the addition of a column-averaged footprint map similar to that in Figure 2c to clarify the complex wind conditions. Given that Figure S9 presents multiple tracks, we will focus on showcasing the two tracks passing over Cairo on August 2, 2022, and November 15, 2022 (represented as Figures S7 and S8, respectively).

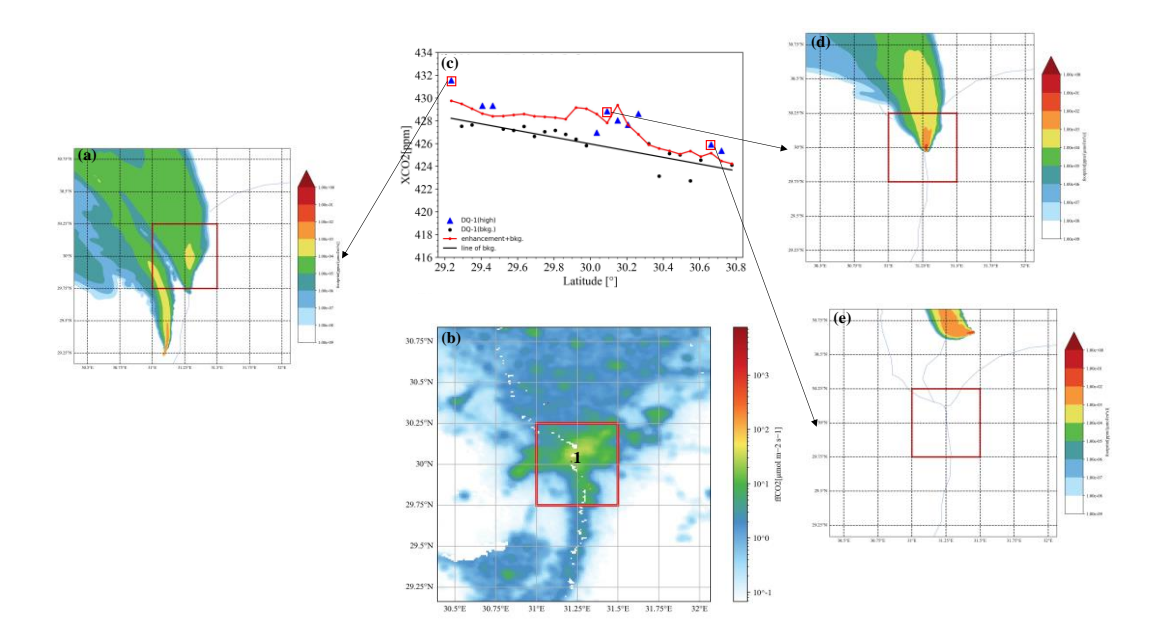


Figure S7. Similar to Figures S5 and S6, XSTILT and enhancement sources are shown for the XCO2 enhancement position of a portion of the DQ-1 orbit transiting Cairo on 15 November 2022 under complex wind conditions

Similar to Figures S5 and S6, Figure S7 presents the column-weighted footprint (X-footprint) simulating fossil fuel emissions and some DQ-1 pseudo-data point locations during the DQ-1 overpass of Cairo. From Figure S7, it can be observed that the simulated XCO2 enhancements within the ranges of 29.2-29.4° and 29.8-30.2° are primarily driven by the main urban emission source 1 (indicated by the red box). The enhancements in the 30.6-30.8° range are attributed to fossil fuel emissions from the northern part of the study area and possibly from sources located just outside the northern boundary of the study region.

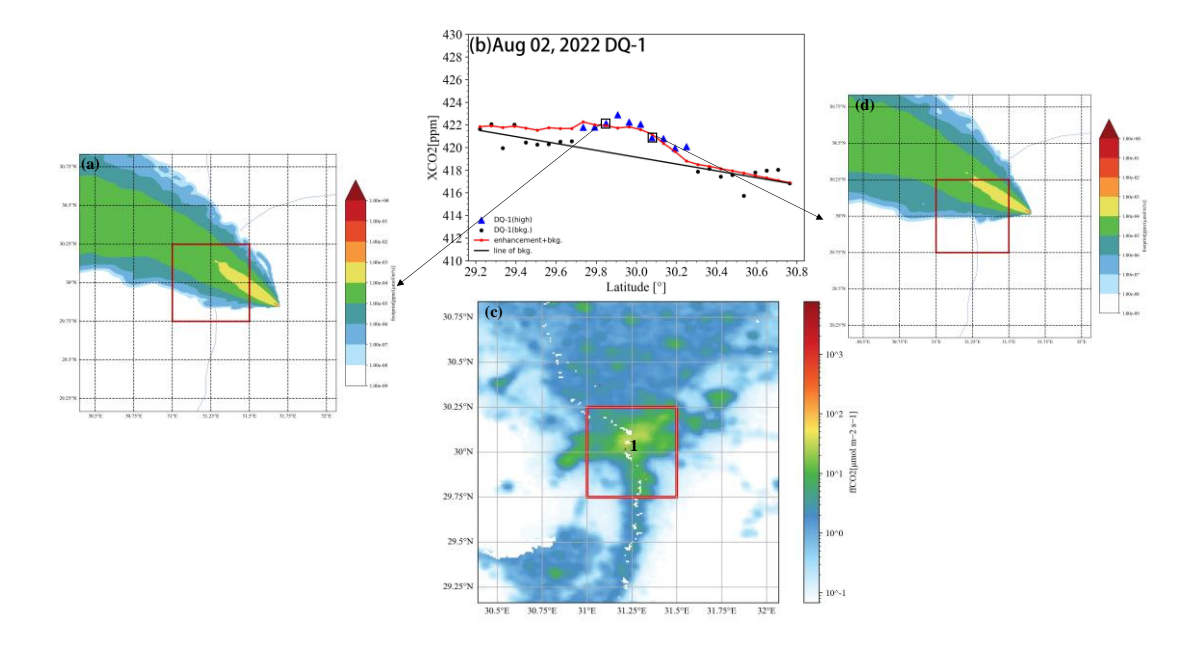
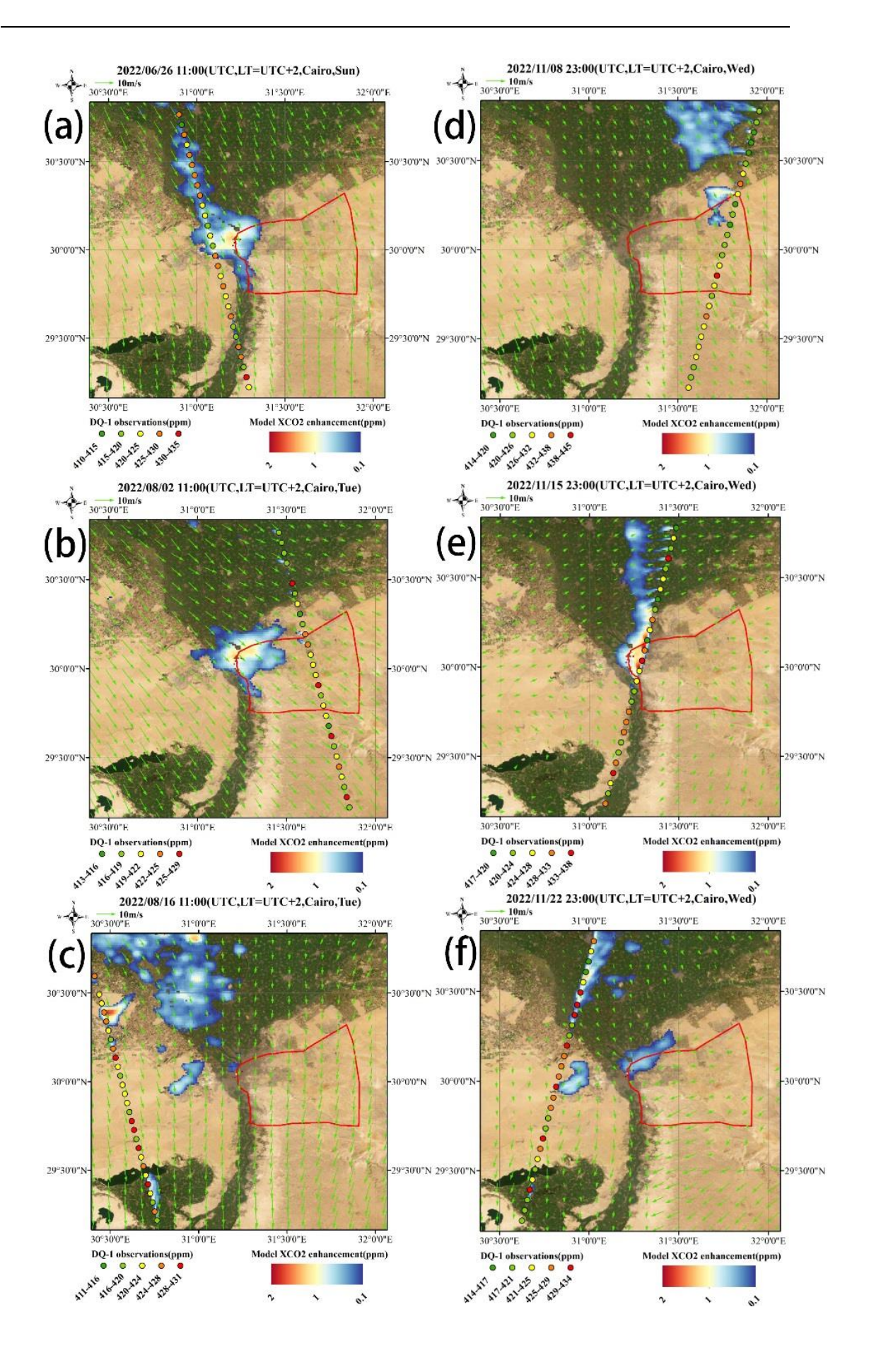


Figure S8. Similar to Figures S5 and S6, XSTILT and enhancement sources are shown for the XCO2 enhancement position of a portion of the DQ-1 orbit transiting Cairo on 02 August 2022 for complex wind conditions

Figure S8 is similar to Figure S7 and clearly demonstrates the impact of the main emission sources in the study area on the XCO2 enhancements observed by DQ-1 and those simulated by the high-resolution atmospheric transport model. Panels a and b indicate that the simulated enhancements in the range of 29.8-30.2° primarily originate from source 1 (red box 1).

You also mentioned that the wind arrows are too small and that there seems to be an error with the color bars: the enhancement values in the left line plot are significantly higher than those in the right colored map. We will enlarge the wind arrows in the revised manuscript. Regarding the color bar issue, we initially aimed for simplicity by combining the simulated plume (colored shading) and the track XCO2 enhancements into a single-color bar. However, since the observed XCO2 enhancement range exceeds that of the simulated plume, it resulted in the discrepancy you noticed. In the revised manuscript, we will create two separate color bars for these components to resolve this issue. Thank you for your careful reading and for pointing out this problem.



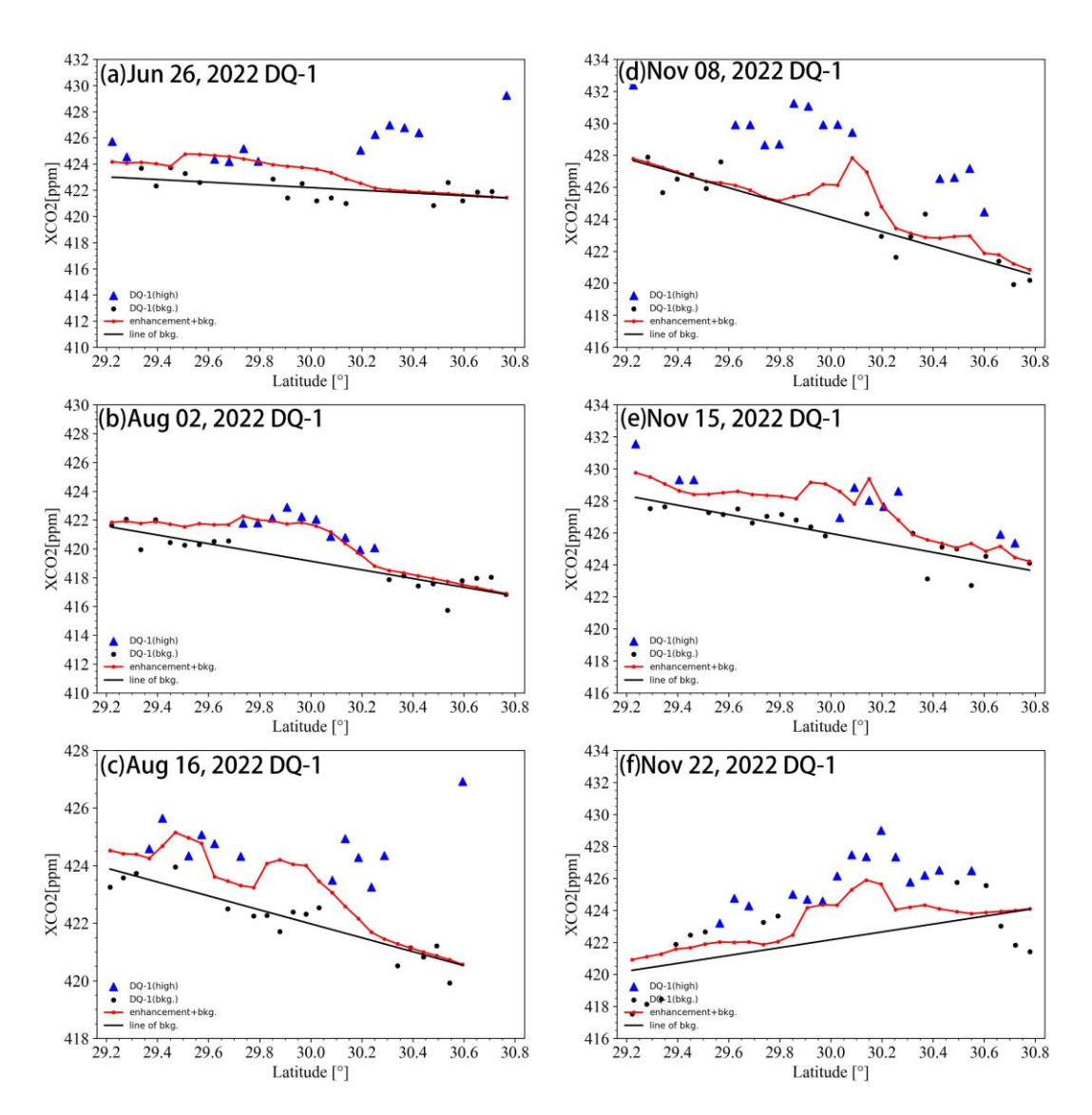


Figure S9-10. Similar to Fig. 3, but for the trajectories of DQ-1 over Cairo on June 26 (Fig.S9-10 a), August 02 (Fig.S9-10 b), August 16 (Fig.S9-10 c) at 11:00 UTC, November 08 (Fig.S9-10 d), November 15 (Fig.S9-10 e), and November 22 (Fig.S9-10 f) at about 23:00 UTC in 2022.

4. Figure 5: The DQ-1 orbit is not visible. The satellite image is too dark. Please mark the city center, the city limits and the TCCON site(s). The figure does not show the wind fields as stated in line 482.

ANSWER: Thank you very much for your suggestions regarding Figure 5 (now Figure 4 in the revised version). You pointed out that the DQ-1 track is not visible, and that the satellite imagery is too dark. We have modified the base map to clearly label the city center and urban boundaries, and we have marked the location of the TCCON station with a red pentagram.

You also noted that the wind field mentioned in line 482 was not displayed. We apologize for the confusion; the wind field referenced is related to line 481, where "The figure" refers to Figure 5, we have revised at Line 493. (Page 19)

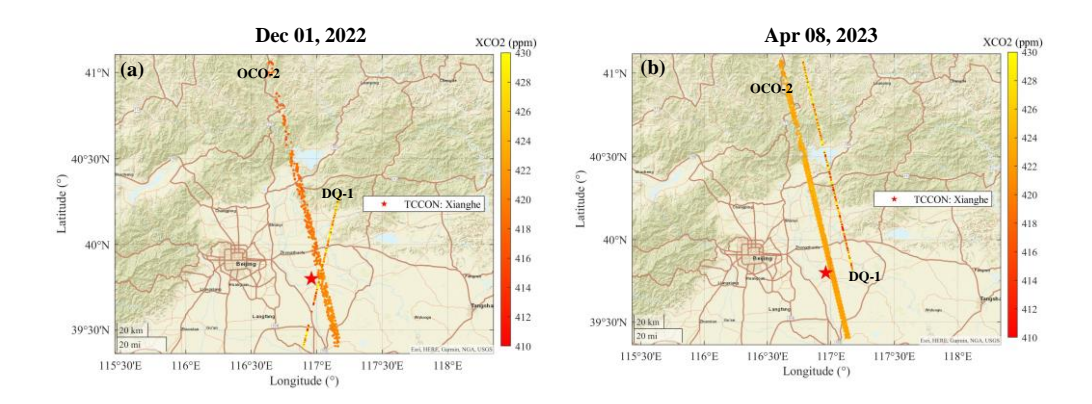


Figure 4: (a) and (b) show the position and XCO2 data of two pairs of OCO-2 and DQ-1 orbits that we selected for transit to Beijing at 05:00 on December 01, 2022 and 05:00 on April 08, 2023, respectively

5.Section 3.3 Estimating Biosphere Fluxes: your statements concerning the natural emissions are based on the examination of very few cases, and thus need to be re-formulated more cautiously. For example, in line 582, only in figure 9d do the simulated enhancements align more closely with the observations, not in the other panels a, b, c. And in line 585, only figure 2c shows that the CASA and ODIAC enhancements differ significantly. Please re-formulate accordingly.

ANSWER: Thank you very much for your suggestions regarding Section 3.3. You pointed out that the statements about natural emissions were based on a limited number of cases and should be phrased more cautiously. We fully agree and have revised the corresponding statements in the revised manuscript accordingly.

Additionally, we appreciate your comment on the inaccuracies in the original description of Figure 9 (now Figure 8 in the revised version). We have corrected this in the manuscript. We now emphasize that the simulations including CASA NEE (blue lines in Figures 8b–d) better match the observed XCO₂ enhancements (black dots) than those driven by fossil fuel emissions alone (red lines). Regarding your note that only Figure 9c (now Figure 8c) shows a clear difference between the CASA and ODIAC enhancements, we have also updated the manuscript to clarify this point and ensure the interpretation is more accurate.

We will revise this section to reflect our findings more accurately regarding the use of diurnal orbits to study the impacts of natural emissions on the inversions. Thank you for your guidance! (Page 26, Line 602-605)

6.References: in about half of all references the journal name is missing and the last author is misspelled. Eldering 2017, Han 2017, Miller 2014, and Wang 2014 are listed twice. In the manuscript, all citations should list only the first author and the year of publication.

ANSWER: Thank you very much for bringing up the errors that appeared in the references, we will check the references one by one in subsequent submissions of the revised manuscript to ensure that each reference meets the requirements of the journal.

Recommended minor changes:

1. line 23: The results of a case study indicate...

ANSWER: Revised (Page 1, Line23)

2. 147: budget of the three fluxes: what do you mean? be more precise

ANSWER: I sincerely thank the reviewers for suggesting a revision to this oversight in the manuscript. Once these background emissions are specified in space and time, the fluxes that are estimated in the inversion process, the "residual" fluxes, represent adjustments to the background fluxes such that the resulting CO2 concentration best matches atmospheric CO2 concentrations observed at particular times and locations. This may be expressed as(Gurney et al., 2005):

$$C_{obs} = C_{ff} + C_{oc} + C_{nbio} + \sum_{i=1}^{N} C_{res}$$

The three fluxes mentioned in line 47 represent C_{ff} , C_{oc} and C_{nbio} .

where C_{obs} represents observed CO2 at a particular points in space and time, C_{ff} represents the contribution to the observed CO2 due to global fossil fuel emissions, C_{oc} , the contribution due to a chosen global oceanic flux, C_{nbio} , the contribution due to a neutral biosphere flux, and C_{res} , the contribution of the residual fluxes from the chosen N discretized regions (Gurney et al., 2000).

We have replaced 'three fluxes' with 'global fossil fuel emission fluxes, choosing global oceanic flux and neutral biosphere flux' in lines 47-49. (Page 2)

3. 149: ...emissions are located.

ANSWER: Revised (Page 2, Line 51)

4. 154 greenhouse gas measurements

ANSWER: Revised (Page 2, Line 55)

5. 185 which is onboard

ANSWER: Revised (Page 4, Line 100)

6. 192 a predetermined conclusion

ANSWER: Revised (Page 3, Line 79)

7. 199 used this tool

ANSWER: Revised (Page 3, Line 86)

8. 1112 fine-scale trace gas transport

ANSWER: Revised (Page 4, Line 112)

9. 1 139 mention the LTAN (local time of ascending node) of DQ-1 to inform on the day/night capacity

ANSWER: DQ-1, as a sun-synchronous orbiting satellite, has a stable daily transit time of approximately 1 p.m. local time during the day and 1 a.m. local time at night. (Page 5, Line 140-141)

10. 1158 integrated weighting function

ANSWER: Revised (Page 6, Line 160)

11. 1189 Atmospheric Model Setting

ANSWER: Revised (Page 8, Line 210)

12. 1 228 of the ACDL product.

ANSWER: Revised (Page 10, Line 250)

13. 1277 described in equations 1 and 2.

ANSWER: Revised (Page 7, Line 176)

14. 1287 the number of dry-air molecules per unit volume

ANSWER: Revised (Page 7, Line 187)

15. 1290 change the XCO2(p) term in the integral on the right side of eq 3 into CO2(p)

ANSWER: Revised (Page 7, Line 190)

16. figure 2: the legends are too small

ANSWER: Revised

17. 1330 and 394: a LEO orbit has a velocity of ~7 km/s, so either you averaged over 7 km, or over 0.5 sec

ANSWER: Line 414 mentions that our pseudo-data was obtained by averaging all the data in one second. We have corrected the error in the manuscript and have now consistently revised all relevant descriptions to "7 km/s or 1 sec" throughout the text.

18. 1387 nighttime observations can also be affected by aerosol and clouds, so explain better what you want to state here

ANSWER: Here is a mistake in our expression, we mean that DQ-1 is different from other passive remote sensing satellites in that it is not only capable of night observation, but also less affected by clouds and aerosols. We'll revise this part of the description in

the revised manuscript. (Page 16, Line 406-407)

19. 1399 Here, sigma represents the random error...

ANSWER: Revised (Page 16, Line 420)

20. 1412 I guess the background XCO2 level is determined by the lidar? Please be more precise.

ANSWER: Here it is a case of sloppy presentation on our part, where background XCO2 level refers to the XCO2 background line derived in Section 2.3.3. Since the derivation of ffXCO2 relies on the observed XCO2 minus the background XCO2, the derivation of ffXCO2 is closely related to the establishment of the background XCO2. (Page 17, Line 434-435)

21. 1485 Figures 6e-h ...

ANSWER: Revised (Page 20, Line 497)

22. 1 648 show these averages in table 1

ANSWER:

Table 1 Results of inversion of urban emission scaling factors for selected cities using DQ-1 XCO2 data

City	Overpass	Prior total emission (Mt C/month)	Prior total emission uncertaint $y(\sigma_a)$	Measurement uncertainty $(\sigma_{measurements}, units: ppm)$	Transport model uncertainty $(\sigma_{Model}, \text{ units: ppm})$	Scaling factor(λ) \pm posterior uncertainty ($\hat{\sigma}$)	OCO-2 Scaling factor/City mean factor
Riyadh	02 March 2023	2.37	45%	1.03	2.53	0.75±0.20	0.80±0.18
	20 June 2022	3.49		0.98	2.58	0.86±0.16	
Beijing	01 December 2022	4.61	25%	1.88/ 2.11	2.64	0.98±0.15	1.09±0.18
	08 April 2023	3.35		1.57/ 1.93	1.79	0.65±0.11	0.70±0.14
	09 January 2023	2.40		2.01	3.04	0.91±0.12	0.83±0.13
	10 January 2023	2.40		1.99	1.45	1.00±0.14	
	19 June 2022	3.81		1.78	2.11	0.96±0.16	
	20 June 2022	3.81		1.52	1.12	0.53±0.11	
Cairo	26 June 2022	2.43	45%	1.08	0.56	1.06±0.20	1.10±0.14
	02 August 2022	2.49		1.45	0.71	0.98±0.12	
	16 August 2022	2.49		1.67	0.87	1.21±0.14	
	08 November 2022	1.96		1.22	0.36	1.15±0.16	

15 November 2022	1.96	0.98	1.31	1.19±0.11
22 November 2022	1.96	1.11	0.21	1.06±0.13

Notes. Scaling factors and their a posteriori uncertainties are shown for each orbit, as well as integrated information for all selected orbits. Uncertainty components are listed for each track, including the a priori uncertainty in the scaling factor and the measurement and transport uncertainty in the integral ffXCO2 (some specific track data inverted using OCO-2 data are bolded, and the average emission scaling factor and a posteriori uncertainty for all tracks in each city are in the last column and highlighted in italics).

23. 1663 45%

ANSWER: Revised (Page 30, Line 687)

24. 1744 June 2022 to April 2023

ANSWER: Revised (Page 36, Line 828)

Reply to Referee # 2

Dear reviewer,

We sincerely thank you for your thorough review and constructive comments on our manuscript. We truly appreciate the time and effort you have invested in evaluating our work. Your insightful suggestions have been very helpful in improving the clarity, depth, and overall quality of our manuscript. We have carefully addressed each of your comments and revised the manuscript accordingly.

This is an important and interesting paper from Yi and co-authors that uses the DQ-1 satellite product to estimate CO2 fluxes from a number of urban areas. The paper is appropriate for publication in ACP with a few changes (detailed below).

There is no data availability section. This is a requirement for publication in ACP as far as I'm aware. The DQ-1 tracks used here should be archived alongside the XCO2 simulated. Please provide links to the OCO-2 and TCCON data used in the analysis, ideally with a DOI. Providing a link to the OCO-2 and TCCON data is important for the continued funding of these projects. What MODIS data was used to scale the NEE products? Please provide a link. As there is no data available, I cannot assess the XCO2 data from DQ-1. So all comments are focused on the method of an analysis, with the assumption that the data underlying it is of sufficient quality to conduct the analysis.

ANSWER: We thank the reviewer for highlighting this important issue. We really appreciate your encouragement and support. In response to your reference to MODIS data for scaling NEE products, we provide an explanation for this: We used Terra Surface Reflectance Daily L2G Global 1km and 500m SIN Grid V061(http://doi.org/10.5067/MODIS/MYD09GA.006). In the revised manuscript, we have added a Data Availability section, now included at the end of the main manuscript, which provides detailed access information for all datasets used in the study:

Data availability

The Level 2 OCO-2 XCO2 data used in this study is archived in permanent repository at NASA's Goddard Space Flight Center's Earth Sciences Data and Information Services Center (GES-DISC) (https://doi.org/10.5067/8E4VLCK16O6Q. The TCCON data used in this study is the GGG2020 **TCCON** the of observations from station Xianghe, (https://doi.org/10.14291/tccon.ggg2020.xianghe01.R0). The CASA-GFED3 NEE data used in this study are archived in repository at NASA's Goddard Space Flight Center's Earth Sciences Data and Information Services Center (GES-DISC) (https://doi.org/10.5067/5MQJ64JTBQ40). NEE data on A Data-driven Upscale Product of Global Gross Primary Production from National Institute for Environmental Studies (Japan) is freely available online at https://doi.org/10.17595/20200227.001. fossil CO2 emission from ODIAC is available online at https://doi.org/10.17595/20170411.001. The MODIS data used in this study is the Terra Surface Reflectance Daily L2G Global 1km and 500m SIN Grid V061(http://doi.org/10.5067/MODIS/MYD09GA.006). The DQ-1 ACDL productions underlying the results presented in this paper are not publicly available at this time but may be obtained from the authors upon reasonable request.

Major Comments:

1. I am a little concerned about the calculation of the background (section 2.3.3). I'm not convinced that DWT is the correct approach to determine the background. Could you test other methods to determine the uncertainty? Maybe some of the OCO-2 approaches and see how much it impacts your result? Do you have enough tracks to ensure the DWT approach is valid?

ANSWER: We have provided a detailed explanation of the discrete wavelet transform (DWT) method for estimating background concentrations in response to the first major comment from Reviewer 1. Additionally, we compared this approach with the method used by Ye et al. (JGR-A, 2020) for calculating OCO-2 background concentrations(Ye et al., 2020). Regarding your concern—"Do you have enough tracks to ensure the DWT approach is valid?"—we applied both the DWT method and the Ye et al. (JGR-A, 2020) approach independently to each satellite overpass. For each case, we derived the corresponding posterior emission factors and associated uncertainties (see Table S3). In Table S3, results derived using the two background estimation methods are highlighted in red when they differ. Notably, only three tracks showed changes in posterior uncertainty, and the posterior emission factors remained identical between the two approaches.

Table S3 Comparison with the OCO-2 Background Method

City	Overpass	Ye et al.'s method(Ye et al., 2020) Scaling factor(λ) \pm posterior uncertainty ($\hat{\sigma}$)	DWT method Scaling factor(λ)±posterior uncertainty ($\hat{\sigma}$)	The whole city emissions (Mt C/month)
Riyadh	02 March 2023	0.75±0.18	0.75±0.20	2.3
	20 June 2022	0.86±0.16	0.86±0.16	3.3
Beijing	01 December 2022	0.98±0.15	0.98±0.15	3.3
	08 April 2023	0.65±0.11	0.65±0.11	2.4
	09 January 2023	0.91±0.12	0.91±0.12	3.5
	10 January 2023	1.00±0.14	1.00±0.14	
	19 June 2022	0.96±0.16	0.96±0.16	2.9
	20 June 2022	0.53±0.12	0.53±0.11	
Cairo	26 June 2022	1.06±0.20	1.06±0.20	2.2
	02 August 2022	0.98±0.12	0.98±0.12	2.4
	16 August 2022	1.21±0.14	1.21±0.14	
	08 November 2022	1.15±0.15	1.15±0.16	1.9
	15 November 2022	1.19±0.11	1.19±0.11	
	22 November 2022	1.06±0.13	1.06±0.13	

2. Atmospheric mixing will magnify the impact of nighttime fluxes on the atmospheric concentration (ecosystem respiration at shallow mixed layer heights) and reduce the impact of daytime flux (photosynthesis at taller mixed layer heights). Eqn 5 must be calculated using the matching hours of the column integrated footprint and the NEE (around Line 309). If the authors think that is not necessary, then they need to include a section showing why that would be the case (it might not be necessary if the biogenic fluxes are too small to matter).

ANSWER: We sincerely appreciate your suggestion regarding the diurnal variation in NEE fluxes. As described in Section 2.3.4, we employed both the CASA model and the ODIAC's NEE product to represent biospheric net ecosystem exchange (NEE), and investigated their influence on fossil fuel flux inversions in Section 3.3.

We fully agree that the time period used for NEE fluxes must be temporally aligned with the column-integrated footprints when simulating XCO₂ enhancements. This has been carefully accounted for in our analysis. Specifically, the CASA NEE product provides 3-hourly fluxes, which we interpret as representative of the current and preceding two hours. Therefore, for each 3-hour NEE window, we use the corresponding hourly footprints for the convolution (inner product) to compute XCO₂ enhancements.

In contrast, the ODIAC's NEE product used in our study does not resolve diurnal variation and provides 10-day averaged NEE values. Accordingly, for each satellite overpass, we used the NEE field closest in time to the overpass date to represent biospheric flux conditions. We will add a clear explanation of this temporal treatment in the revised manuscript to enhance clarity and transparency.

3. I commend the authors for investigating the horizontal transport of the footprints (around Line 338). But the atmospheric concentrations calculated from footprints (convolved with inventories) are highly sensitive to the height that the emissions are mixed up to (known as mixed layer height (MLH), which is a variable in the STILT configuration setup. This uncertainty is much larger at night as the top of the nocturnal boundary layer begins to reduce in altitude. The authors might want to quantify how sensitive the calculated footprints (and hence fluxes) are to that change in MLH at night. There is a similar magnitude of changes in the MLH between winter and summer days.

ANSWER: We sincerely thank you for your recognition of our work, as well as for highlighting the importance of nighttime and seasonal variations in the mixing layer height (MLH) on STILT-based inversions. In our study, we use the term "Planetary Boundary Layer Height (PBLH)," which is closely related to MLH and commonly used in the context of atmospheric transport modeling. For consistency, we will refer to PBLH throughout the manuscript and provide a clarification in the methods section that PBLH is used interchangeably with MLH in this context. In response, we will incorporate an additional subsection in the discussion section dedicated to a sensitivity analysis of inversion results with respect to MLH variability.

Vertical turbulent mixing, as the dominant process governing the vertical transport of air parcels, regulates the dilution of surface emissions within the planetary boundary layer (PBL). Uncertainties in vertical mixing or PBL height can influence both the magnitude and spatial distribution of atmospheric footprints through variations in horizontal advection at different altitudes (Gerbig et al., 2008). Variations in the STILT-modeled mixed layer height alter the vertical profiles of turbulent statistics that govern the stochastic motion of Lagrangian air parcels (Lin et al., 2003), thereby

yielding distinct air parcel trajectories under different PBL height.

In this section, we assess the sensitivity of both horizontal footprints and column-averaged footprints (X-STILT) to variations in the planetary boundary layer height (PBLH) as simulated by STILT. Given the pronounced diurnal and seasonal variability of terrestrial PBLH across most latitudes(Gu et al., 2020), we selected three satellite overpasses across Beijing to quantitatively evaluate the impact of PBLH on footprint estimates: 23:00 on 9 January 2023 (winter nighttime), 05:00 on 10 January 2023 (winter daytime), and 23:00 on 19 June 2022 (summer nighttime). For each overpass, the location (latitude and longitude) corresponding to the largest modeled XCO₂ enhancement along the track was selected as the receptor location for STILT, with release heights consistent with prior model configurations. Backward simulations were conducted from the overpass time until local sunrise or sunset (sunset for nighttime passes and sunrise for daytime passes). A range of PBLH values from 300 m to 1500 m, in 200 m increments, was tested.

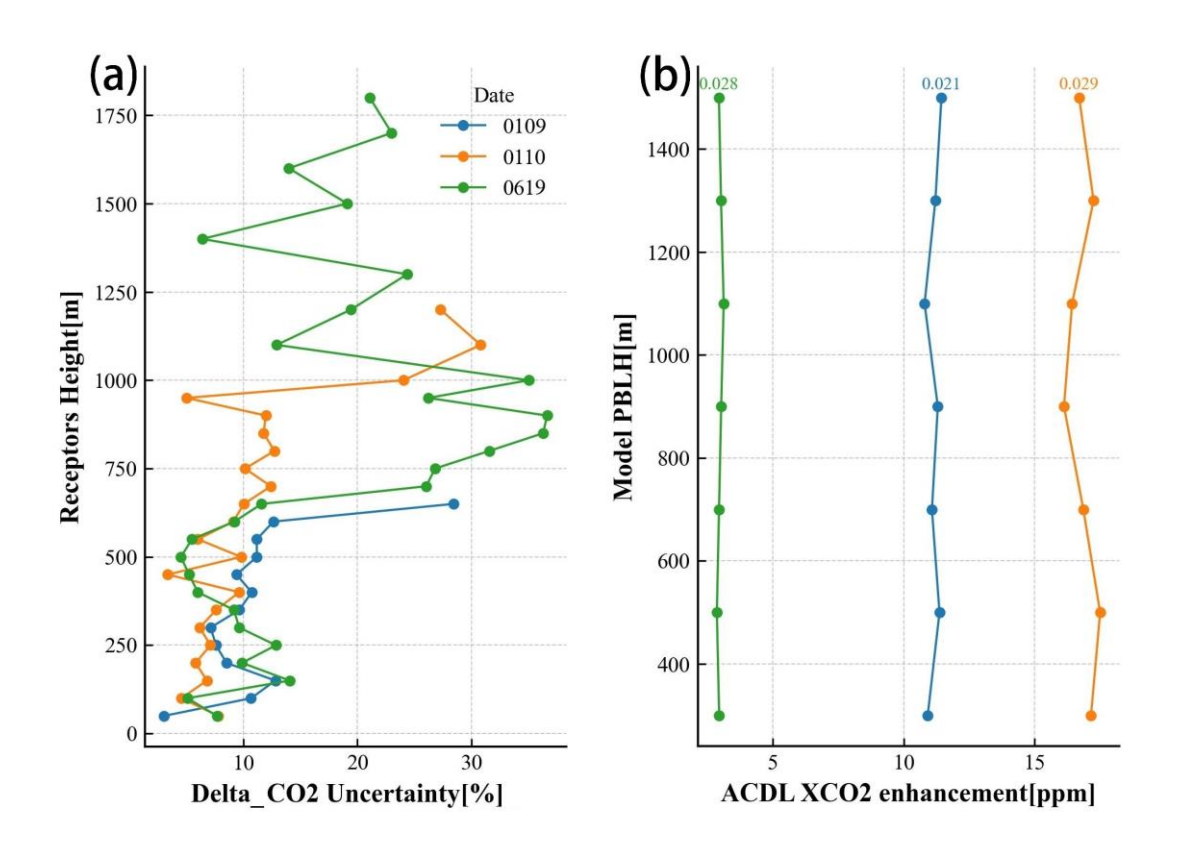


Figure 10: Panels a and b illustrate the sensitivity of CO₂ and XCO₂ enhancements to variations in planetary boundary layer height (PBLH) at different receptor altitudes, quantified by the coefficient of variation (i.e., the standard deviation divided by the mean). Panel a presents the simulated results for three satellite overpasses: 23:00 on 9 January 2023 (winter night, blue line), 05:00 on 10 January 2023 (winter day, orange line), and 23:00 on 19 June 2022 (summer night, green line). For each case, receptors were placed at the locations of maximum modeled XCO₂ enhancement along the satellite track, with release heights consistent with prior STILT configurations. Panel b shows the corresponding XCO₂ enhancement simulations for each date, with the coefficient of variation annotated at the top of the panel to indicate the overall sensitivity across varying PBLH scenarios.

Figure 10a illustrates the sensitivity of modeled XCO2 enhancements—calculated following the method in Section 2.4.1—to varying PBLH values at different release heights for three selected receptors. The x-axis, labeled Delta XCO₂ Uncertainty, quantifies this sensitivity as the coefficient of variation (standard deviation divided by the mean) of XCO2 enhancements obtained from simulations with different PBLH values at the same release height. A higher value indicates a stronger response of the modeled enhancement to changes in PBLH. Results in Figure 10a show that on the nighttime overpass of 9 January 2023 (blue line), the relative variation in modeled XCO₂ enhancements remains within ~10% for release heights below 600 m and does not exceed 13%, with a minimum of 3.03% at 50 m. Similarly, for the daytime overpass on 10 January 2023 (orange line), relative variations remain below 13% up to 950 m, with a minimum of 3.36% at 450 m. Notably, for this pair of consecutive day-night overpasses, nighttime sensitivity is generally higher than daytime at release heights below 650 m. The nighttime overpass on 19 June 2022 (green line) exhibits a broader vertical range of valid footprints—unlike the 9 January case, where no valid footprints were simulated above 650 m, possibly due to seasonal effects. This case also shows a stronger dependence on PBLH at higher altitudes, particularly between 750-1000 m, with the maximum sensitivity reaching 36.6% at 900 m. Overall, our findings suggest that within the lower troposphere and across the selected case studies, the influence of PBLH variability on modeled XCO₂ enhancements is generally on the order of 10%, increasing with receptor altitude. As columnaveraged observations are less sensitive to the vertical distribution of air parcels(Lauvaux and Davis, 2014), the sensitivity of modeled column XCO2 enhancements to PBLH variations is notably smaller. This is corroborated by Figure 10b, which shows modeled XCO2 enhancements as a function of PBLH for each overpass, with corresponding coefficients of variation annotated above the lines: 2.1% (9 January), 2.9% (10 January), and 2.8% (19 June)—all lower than the minimum values observed in Figure 10a.

Given that ACDL is equipped with an aerosol channel, it can provide extinction coefficient profiles and planetary boundary layer height (PBLH) products(Dai et al., 2024). In this study, we utilized ACDL-retrieved PBLH data for forward simulations, which helps to mitigate errors associated with inaccurate PBLH settings. Moreover, since satellite measurements represent column-averaged concentrations, they are inherently less sensitive to variations in PBLH. Therefore, we conclude that PBLH has a negligible impact on the inversion results presented in this study.

4. Shekar et al 2020's study of the Nile River Delta (slightly larger domain but includes the area here) show large NEE from agriculture in summers north of Cairo. They find that ODIAC (and EDGAR) are vastly underestimating FF CO2. Why do you think they get a different result? Should you include the NEE for Cairo too? They also point out that "Burri et al (2009) measured CO2 fluxes using the eddy covariance method at the University of Cairo and showed that the CO2 fluxes have a significant diurnal and weekly variation, with peak CO2 flux occurring between 14:00 and 16:00 and minimum flux on Friday (rest day due to Muslim prayer day on Friday)". Do you know what day of the week the DQ-1 Observations were made in each of the cities?

ANSWER: We appreciate the reviewer's thoughtful comment and the reference to (Shekhar et al., 2020). In their study, Shekhar et al. (2020) compared XCO₂ enhancements observed by OCO-2 over 32 days from 2014 to 2019 with modelled XCO₂ enhancements derived from emission inventories and the STILT transport model. They reported a mean emission factor (MEF)—defined as the ratio

of the mean observed enhancement to the mean modelled enhancement across all days—of 3.36 (3.19–3.45) for ODIAC, concluding that ODIAC substantially underestimated fossil fuel CO₂ emissions in the Nile Delta region (which encompasses our study area). Similarly, as discussed in Section 4.1 of our study, we also found that ODIAC underestimates fossil fuel emissions over Cairo.

While both studies utilize satellite observations to optimize prior emission estimates, there are several key methodological differences between our approach and that of Shekhar et al. (2020), particularly in background calculation, inversion framework, and prior uncertainty configuration. Specifically, Shekhar et al. (2020) derived a constant background XCO₂ value for each OCO-2 track by selecting data within a 1° latitude band over the desert that had not been influenced by the Nile Delta, and applied this value uniformly along the entire track. In contrast, we employed a discrete wavelet transform (DWT) combined with linear regression to derive a latitudinally varying background, which we refer to as $XCO2_{trend}$ in Section 2.3.3. Our background line was not derived from a "clean" reference region but instead captures the components of XCO₂ not attributable to fossil fuel emissions.

Furthermore, we used a Bayesian inversion framework to optimize the prior emission field over the entire study domain, resulting in posterior scaling factors derived from Bayesian optimal estimation, along with associated posterior uncertainties. In contrast, Shekhar et al. (2020) characterized underestimation using the MEF metric. Therefore, the definition and computation of the emission factors differ significantly between the two studies.

As detailed in Section 2.4.2, previous studies have evaluated the prior uncertainty in ODIAC emissions for urban inversions. Given the industrial nature and irregular emission characteristics of cities like Cairo and Riyadh—where biospheric fluxes are negligible and industrial emissions are highly uncertain—we assigned a 45% prior uncertainty for fossil fuel emissions in these cities.

Regarding the reviewer's question on the contribution of NEE from agricultural regions north of Cairo—particularly during summer, when biospheric uptake can be substantial—we addressed this concern in Section 2.3.3. Since our background values are designed to isolate the fossil-fuel-driven component of XCO₂ enhancements, and considering our study domain is spatially limited and uses constant lateral boundary conditions in the simulation, we assume that any XCO₂ signal associated with biospheric activity (including NEE) is incorporated into the background term.

We have added the day-of-week information for each DQ-1 track in Figures 3, 5, 7, and S9. Furthermore, in Section 3.4, we cited the work of Shekhar et al. (2020), highlighting that our findings in Cairo are consistent with theirs—both studies indicate that ODIAC underestimates fossil fuel CO₂ emissions in the city.

Minor comments:

Line 10: You need to define CO2 the first time it's used: total column dry-air carbon dioxide (XCO2). Make sure all CO2 is subscript.

ANSWER: Revised (Page 1, Line 10).

Make sure to sort out the citations throughout the manuscript. And each paragraph should have an indent. But I assume copyediting will catch all that.

ANSWER: Revised (Section References, Page)

line 18: define ODIAC. Or you could just say that the inventory overestimated...

ANSWER: Revised (Page 1, Line 18).

Line 37: "the booming economics" is not correct. I would suggest something like "their rapidly growing/changing economies".

ANSWER: Revised (Page 2, Line 37)

line 47: the "three" fluxes here was confusing. I think your response to Review 1 was sufficient.

ANSWER: We thank the reviewer for the kind note and for acknowledging our response to Reviewer 1. In the revised manuscript, we have clarified the wording around the "three fluxes" on line 47 (Page 2) to ensure it is more intuitive to readers. We appreciate your careful attention to clarity and your positive assessment of our prior explanation (Page 2, Line 47-49).

line 62: "map the gross primary production" doesn't make sense to me. I think you mean something like "map the net CO2 uptake by the biosphere". If that's the case, I would recommend changing that wording.

ANSWER: We thank the reviewer for this helpful suggestion. Indeed, our original wording was imprecise. We intended to refer to the net CO₂ uptake by the biosphere, not gross primary production per se. We appreciate your careful reading and thoughtful recommendation (Page 2, Line 63).

Line 68: Define LIDAR the first time it's used. "are ambitious" is not used correctly here. You could say "ambitiously planned" or something like that.

ANSWER: Revised (Page 3, Line 68-69)

Line 72: Define CO2-IPDA.

ANSWER: Revised (Page 3, Line 72-73)

Line 77: You could start a new paragraph here and the text would flow better.

ANSWER: Revised (Page 3, Line 78)

Line 84: Define ACDL.

ANSWER: Revised (Page 4, Line 100)

Line 87: "figure out" is not formal enough. Use something like determine, quantify, etc

ANSWER: Revised (Page 4, Line 103)

Line 91: It feels like this paragraph should come before the LIDAR discussion.

ANSWER: Revised (Page 3, Line 78-92)

Line 99: "several scientists utilized this effect tool..." should be "several studies used this tool..."

ANSWER: Revised (Page 3, Line 86)

line 115: provided should be calculated or simulated

ANSWER: Revised (Page 4, Line 115)

Line 157: It would be easier to interpret the results presented later if all the relevant info about the DQ-1 configuration were together. A quick summary of the ground sampling configuration (I believe it's a 70m diameter circle sampled every 350m), frequency of overpass (how often could we image these cities in an ideal scenario?), is the track sampling from north to south or south to north? The day/night local overpass time, etc. All the info that is spread across the manuscript but could be summarized so the reader can appreciate the strength of the data.

ANSWER: We thank the reviewer for the helpful suggestion. To improve clarity and provide a consolidated summary of the DQ-1 satellite configuration, we have added a new table (Table S1) in the Supplementary Information.

Table S1 Several primary parameters of ACDL(Fan et al., 2024)

Parameters	Values		
Oribit altitude	705km		
Lidar footprint diameter	~70m		
Horizontal spacing of lidar footprints	~350m		
Field of view	<0.2mrad		
Telescope diameter	1000nm		
Divergence angle after laser beam expansion	<0.1mrad		
Repetition frequency	20Hz		
Laser pulse width	<50ns		
Laser energy	75mJ		
Off-line wavelength	1572.085nm		
On-line wavelength	1572.024nm		

line 165: Define WF.

ANSWER: Revised (Page 6, Line 167)

Line 212: what configuration of STILT was used? Did you use the default configuration from STILT v1 or v2? I can't remember what X-STILT uses but it should be mentioned. What is the ground spatial resolution of the gridded STILT footprints? Are you using the hourly column integrated footprints or a summed 24 hour column integrated footprint (which will be a problem for NEE, see above).

ANSWER: Thank you very much for your valuable suggestions. We used STILT version 2 and XSTILT version 1 in this study, and the versions of all models employed are listed in the Supplement (see Table S2). The ground spatial resolution of the STILT footprints is $1 \text{ km} \times 1 \text{ km}$. The simulations

for Riyadh, Cairo, and Beijing presented in Sections 3.1 and 3.2 use footprints integrated over a 24-hour period. In Section 3.3, simulations incorporating CASA NEE data use hourly footprints matched to the corresponding NEE time, while those incorporating ODIAC NEE data employ footprints integrated over an 8-hour period. We will clarify these details in the respective sections of the manuscript. (Page 17, Line 436. Page 25 Line 583-585)

Table S2 Model version information used in this study.

Model	Version
STILT(Stochastic Time-Inverted Lagrangian Transport)	V2
WRF(Weather Research and Forecasting)	V4.0
X-STILT(X-Stochastic Time-Inverted Lagrangian Transport	VI
model)(Wu et al., 2018)	

line 219: The Hefner and Gilfillan citations are both incomplete. Is this from a journal? What is the DOI?

ANSWER: Revised

line 250: I would change "biological flux" to Biogenic carbon flux. I assume you're not including human respiration in your estimates of CO2 flux for these cities so Biological flux is not accurate. I think biogenic is a more appropriate word here.

ANSWER: Revised (Page 11, Line 276)

What were the meteorological conditions for each city during the DQ-1 overpass? Was the vegetation active all year round (as might be in the tropics) or was the vegetation dormant in the Beijing winter?

ANSWER: We present partial meteorological conditions during the DQ-1 overpass periods and indicate whether vegetation is dormant during winter in the overpassed cities in Table S4 of the Supplement.

Table S4 DQ-1 Orbital transit meteorological conditions

City	Overpass	Humidity (%)	Barometer (mbar)	Weather	Temperature (°C)	Vegetation Dormant
Riyadh	02 March 2023	24	1019	Passing clouds	29/13	No
	20 June 2022	7	1004	Sunny	46/28	
Beijing	01 December 2022	18	1033	Haze	0/-7	Yes
	08 April 2023	37	1004	Haze	24/8	

	09 January 2023	52	1031	Sunny	7/-6	
	10 January 2023	19	1026	Sunny	7/-6	
	19 June 2022	72	1002	Haze	34/23	
	20 June 2022	52	998	Cloudy	34/23	
Cairo	26 June 2022	27	1010	Sunny	35/23	No
	02 August 2022	40	1005	Passing clouds	35/26	
	16 August 2022	40	1009	Sunny	33/25	
	08 November 2022	68	1014	Clear	25/19	
	15 November 2022	72	1018	Haze	23/17	
	22 November 2022	82	1016	Fog	24/18	

Note: Historical weather data were retrieved from Timeanddate.com, which uses CustomWeather sourced from WMO-certified airport stations and MADIS community stations, with update intervals ranging from 30 min to hourly (https://www.timeanddate.com/weather).

What is the spatial resolution of the NEE? GFED4 has been released for years. Is there a reason you are using GFED3?

ANSWER: We considered using GFED4 but ultimately chose GFED3 because the GFED4 dataset provides global estimates of monthly burned area, monthly emissions and fractional contributions of different fire types, daily or 3-hourly fields to scale the monthly emissions to higher temporal resolutions, and data for monthly biosphere fluxes. However, GFED4 does not directly provide three-hourly NEE data, which is why we selected GFED3 for our study. The spatial resolution of the NEE data used in our study has been specified in the revised manuscript (CASA NEE $0.5^{\circ} \times 0.625^{\circ}$ and ODIAC NEE $0.1^{\circ} \times 0.1^{\circ}$). (Page 11, Line 288-289)

Line 263: what is the spatial resolution of the MODIS Green vegetation product you used? Is there a link to this product? (Include it in the data availability section too). Did you use year specific products or a compilation of many years?

ANSWER: We used MODIS climate data (Terra Surface Reflectance Daily L2G Global 1km and 500m SIN Grid V061 http://doi.org/10.5067/MODIS/MYD09GA.006) from 2010 to 2020 (with a spatial resolution of 500 m \times 500 m) to derive the Green Vegetation Fraction (GVF). The data link has been provided in the Data Availability section.

Line 275: include the wavelengths to clarify the on and off-wavelengths

ANSWER: Revised (Page 5-6, Line 148-149)

Line 282: TOA not top.

ANSWER: Revised (Page 7, Line 181)

Line 291: I found the title of section 2.4.1 really confusing. I would suggest that the authors separate

out the LIDAR observations (very important on their own) from the combination of STILT footprints with the inventories to create the simulated XCO2.

ANSWER: Thank you very much for your valuable suggestion regarding the structure of our manuscript. In response, we have revised the presentation by separating the description of the LIDAR observations from the STILT footprint and emission inventory-based XCO₂ simulations. Specifically, the content related to the LIDAR observations has been moved to Section 2.1 to improve clarity and coherence. (Page 7, Line 172-190)

Line 324. The terminology is difficult to follow in this section. The observed enhancement above background dXCO2, has been labeled as ff only. But there is not enough information available to conclude that all the emissions are fossil fuel only (biogenic, human respiration, etc). Instead of using ffXCO2_p, you could use dXCO2_obs. It would be less confusing for the reader. Using p and a for observed and simulated is also confusing to follow. You could use obs and sim as subscripts instead and it would be easier to follow.

ANSWER: We have revised all subscripts throughout the revised manuscript in accordance with your request. Thank you for pointing this out.

line 337: Start a new paragraph for the transport model.

ANSWER: Revised (Page 14, Line 358)

Line 366: The satellites don't measure fluxes, they are calculated from the concentrations. So the wording here should be "such as those created using high-res..."

ANSWER: Revised (Page 15, Line 386)

Line 391: What about NEE? Should that have been included too?

ANSWER: We have incorporated NEE into our discussion and provided an explanation in Line 412 of the revised manuscript. Thank you for your valuable suggestion. (Page 16, Line 412)

Line 409: which months? Is there a table of these results some where?

ANSWER: We have consolidated the specific overpass dates of each orbit and the monthly total posterior emissions for the corresponding cities in Table S3 of the Supplement. (Page 17, Line 431-432)

Line 416: The variable labelled "ffXCO2 observed enhancement" is actually the observed XCO2 enhancement with the assumption that ALL of the CO2 is from fossil fuel sources. I disagree with that assumption. While most of the CO2 will be from FF, there will also be CO2 from human respiration and biogenic fluxes could be non-zero in these cities. There is better use of the terminology in the discussion that could be used here.

ANSWER: We have replaced the terminology here with the terms used consistently in the Discussion section. (Page 17, Line 439)

Line 428: Are the wind speed shown in Fig 3 the instantaneous winds at the time of the overpass or the mean winds from WRF?

ANSWER: We used average wind speed simulated by WRF. (Page 18, Line 450-451)

Line 432: Please specify the time zone. I assume this is 11am UTC? I would also ask for the local time alongside the UTC. It will make it easier for the reader to follow when it comes to interpreting the results.

ANSWER: We have used Coordinated Universal Time (UTC) throughout the manuscript. In the revised version, we have added the corresponding local time information to Figures 3, 5, and 7 for clarity.

Line 439: "Better" seems generic. Could you be more specific here?

ANSWER: We have revised the description in line 439 to improve clarity and accuracy: Compared to the track on March 2, the track on June 20 shows better agreement between observations and simulations, along with smaller posterior uncertainties (see Table 1). Thank you for your suggestion. (Page 18, Line 462-463)

Line 443: I assume ffXCO2 is observed? I would specify that here.

ANSWER: Revised (Page 18, Line 466)

Figure 4: Most of the text on the figures is too small to see but Fig 4 is really difficult. I would recommend splitting it over two lines and make everything a little bigger. Fig 6 is easier to see.

ANSWER: Thank you for your valuable suggestion. Considering that there are many tracks over Cairo, displaying all of them in the main manuscript would occupy substantial space. Therefore, we have moved the original Figure 4 from the main text to the Supplement, where it is now presented as Figures S9 and S10 for completeness.

This is more of a suggestion, than a requirement, but something I have found useful is to show figures with latitude on the Y axis, and the other variable on the X axis. So it would mean that figures with XCO2 vs Latitude are rotated to match the maps. I know that's not the normal way to do it, but it would make it easier for the reader to follow the flight track of the satellite and match the XCO2 vs Latitude to the maps. I would also suggest indicating the outline of the city in shading in the background on these graphs if it's not there.

ANSWER: We thank the reviewer for this helpful suggestion. We agree that aligning the figures more closely with the map orientation could aid interpretation. However, we have chosen to retain the current layout, as presenting XCO₂ along the satellite track direction preserves the native resolution and continuity of the measurements, which is crucial for interpreting the observed enhancements. Regarding the city boundaries, these are already indicated in the figures where relevant, and we have further clarified this in the revised captions to ensure visibility. We hope the reviewer finds this presentation acceptable.

Line 452: Instead of Compared to, I think you mean In contrast to.

ANSWER: Revised (Page 18, Line 472)

Line 458: similar in space? Maybe clarify how they are similar.

ANSWER: We have included an explanation regarding this adjustment in the revised manuscript.

"The latitudinal distribution and magnitude of the simulated enhancement (red line) are generally consistent with those of the observed enhancement (blue triangles)" (Page 19, Line 478-480)

Line 459: overlooked -> did not include

ANSWER: Revised (Page 19, Line 480)

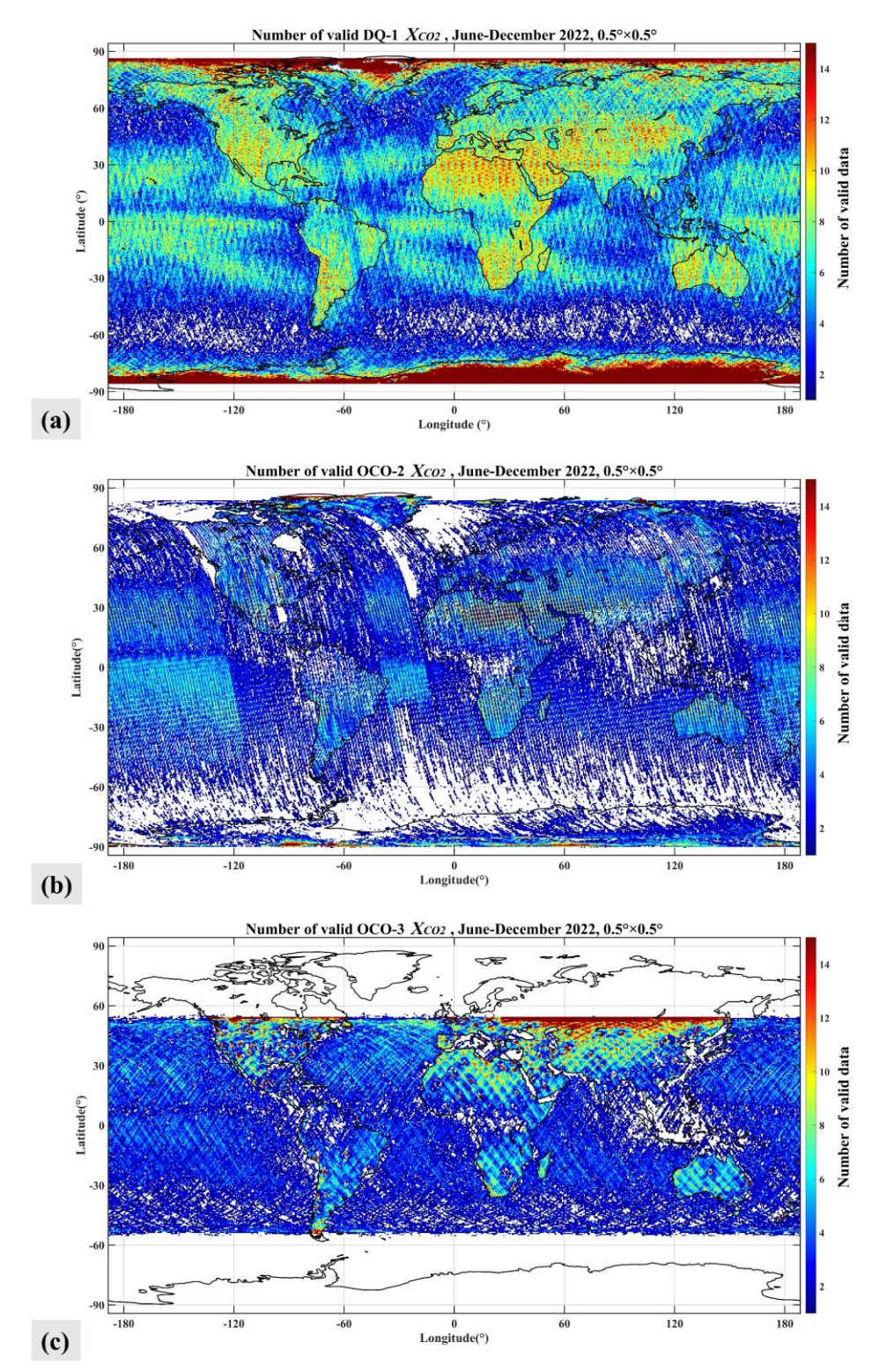
Line 460: Were there any problems with the sand/dust/aerosols? Given the paper has focused on cities with high aerosol loadings, it might be worth saying more about how that is not a problem for the lidar vs other CO2 satellites.

ANSWER: In our previous study(Han et al., 2024), we conducted a global data completeness comparison between DQ-1 and OCO-2/3 under high aerosol optical depth (AOD) conditions to demonstrate DQ-1's capability for observations in such environments. We also compared observational examples from a DQ-1 track and an OCO-3 track over the North China Plain, which includes our Beijing study area, under high AOD conditions.

Fig 5: I like this for Beijing. Could you do the same for the other cities? It would provide context for the readers that seems to be missing.

ANSWER: We have revised Figures 3, 4, 6, and 8 following the style of Figure 5. Specifically, Figures 4 has been moved to the Supplementary Materials as Figures S9 and S10, while Figures 3, 6, and 8 in the original manuscript are now numbered as Figures 3, 5, and 7 in the revised version.

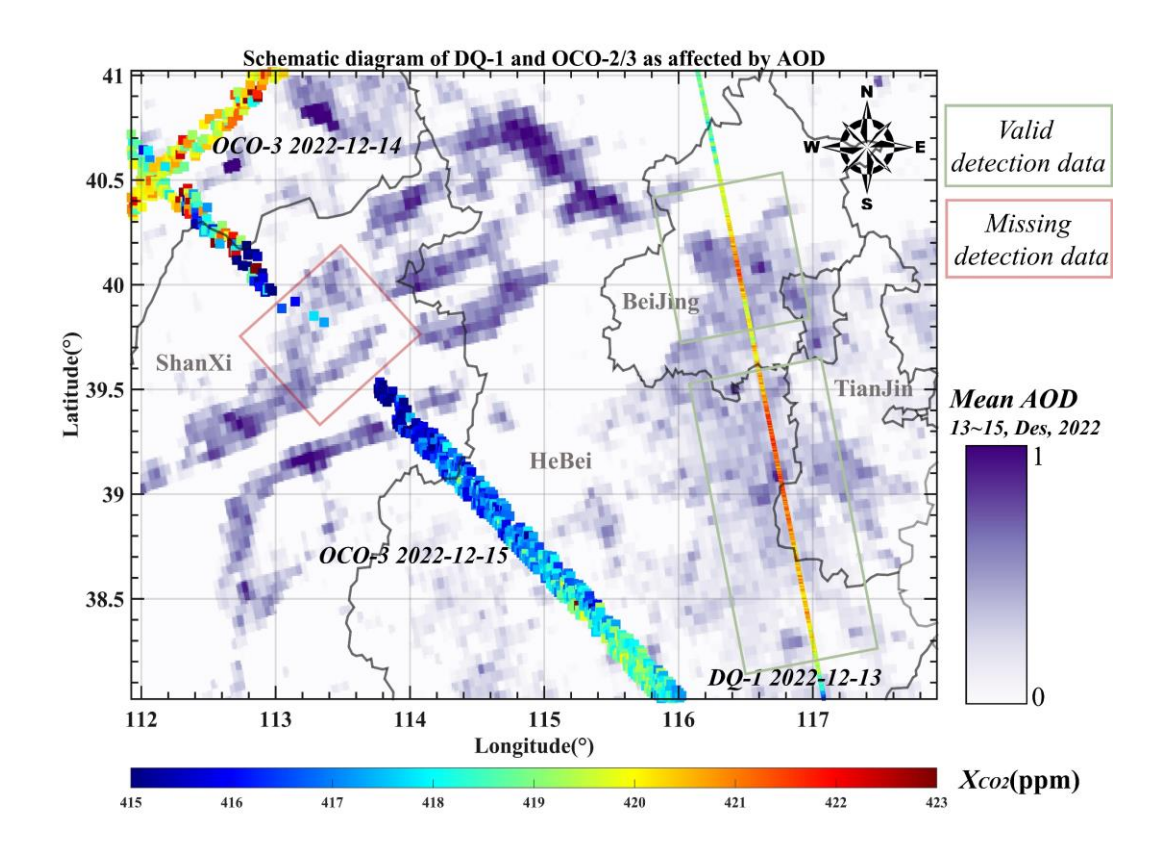
The capability of the DQ-1 laser detection satellite to observe XCO2 at night and under high Aerosol Optical Depth (AOD) conditions is crucial for complementing traditional optical satellites such as OCO-2 and OCO-3. To demonstrate the advantages of ACDL compared to optical satellites, we downloaded global observation data from OCO-2 and OCO-3, as well as MODIS AOD retrieval data for the same period, from the NASA website (https://search.earthdata.nasa.gov/search). Figure 11 compares the spatial coverage of valid observations on a 0.5° resolution grid by DQ-1, OCO-2, and OCO-3 from June 1 to December 31, 2022. Due to its orbital inclination, OCO-3 cannot observe high latitude regions, whereas both OCO-2 and DQ-1 have polar orbits. It is evident that the effective observation density of DQ-1 is significantly higher than that of OCO-2 and OCO-3 globally, especially over the Northern Hemisphere land. The proportion of grids with at least one valid detection by DQ-1 reached 87.6%, while OCO-2 and OCO-3 only achieved 66.2% and 50.8%, respectively. Even the combined observations of OCO-2/3 reached only 74.8%.



Note: Comparison of the coverage maps of the number of valid observations from DQ-1, OCO-2, and OCO-3 on a 0.5° grid from June 1 to December 31, 2022.

In northern China, specifically in the Shanxi, Shandong, and Beijing-Tianjin-Hebei regions, AOD is relatively high, particularly in winter when smog and other weather conditions are common(Yang et al., 2019). The CO2 emissions from power plants across the entire North China Plain are comparable to those of the entire Netherlands(Du et al., 2018). Missing data under high AOD conditions can result in significant deviations in emission factor calculations. Figure 12 shows the

effective detection results of OCO-3 and DQ-1 passing over the high AOD regions of northern China from December 13 to 15, 2022. On December 15, OCO-3's pass over the high AOD region in Shanxi province resulted in a noticeable lack of observational data, as indicated by the red box in the figure. In contrast, DQ-1's sub-satellite track over Beijing and Tianjin maintained data continuity while also detecting two significant enhancements, as highlighted by the green box in Figure 12.



Note: Comparison of Effective Detections of OCO-3 and DQ-1 Over High AOD Regions from December 13 to 15, 2022, with the Base Map Showing AOD Retrieval Values Provided by MODIS.

Line 469: Should this paragraph be in the methods?

ANSWER: We have incorporated this paragraph into Section 2.4.1 in the revised manuscript. (Page 12-13, Line 321-330)

Line 485: Fig 5 only has a,b. Do you mean Fig 6?

ANSWER: We sincerely thank you for pointing out this error. According to the original figure numbering, it should indeed be "Fig. 6 (e)–(h)". However, since we have moved Figure 4 to the Supplementary Materials, we have chosen to keep the current numbering in the main text for consistency and clarity.

Line 505: But do DQ-1 and OCO-2 show the same spatial trends? Would be worth including that point here.

ANSWER: We have added a discussion here regarding whether DQ-1 and OCO-2 exhibit consistent spatial trends.

On 1 December, both the DQ-1 and OCO-2 overpasses exhibited similarly strong latitudinal

gradients in their background baselines, with notable enhancements observed and simulated within the 39.4°–39.6°N range. Although the background latitudinal gradients differed between DQ-1 and OCO-2 on 8 April, both were weak in magnitude, and significant enhancements were nevertheless consistently detected and simulated between 40.0° and 40.4°N. (Page 22, Line 516-521)

Line 544: Agree. Hence needing hourly convolutions of NEE and footprints.

ANSWER: Revised

Line 559: "Forward eight-hour". I would phrase it as the previous 8 hours before the overflight.

ANSWER: Revised (Page 25, Line 576)

Line 564: Start a new paragraph.

ANSWER: Revised

Line 566: Shouldn't you use the same method as previously? How is this different?

ANSWER: We used the background calculation method described in Section 2.3.3 to separate the observed DQ-1 XCO₂ into XCO₂ trend and XCO₂ local components. The background line with a latitudinal gradient was derived using discrete wavelet transform (DWT) combined with linear regression. We consider this background to include the XCO₂ enhancements caused by net ecosystem exchange (NEE). However, for the purpose of quantifying the impact of NEE on emission inversion in this section, we selected the minimum values from the pseudo-data along each orbit as the background concentration. This approach results in XCO₂ enhancements that encompass contributions from both fossil fuel emissions and NEE.

Line 590: absorption phenomenon? I think you mean CO2 uptake or depletion. I would not use absorption to indicate a carbon flux when you were already talking about it as part of the retrieval process. Same on line 593.

ANSWER: Revised (Page 26, Line 610, 613)

Figure 9: Why is panel (b) not over the same latitude range? I also really like the terminology used in Figure 9 and the description. This is the kind of terminology that should be used in the methods section for the description of the STILT footprints x inventory discussion.

ANSWER: The latitudinal range of the orbit shown in Figure 9(b) is narrower compared to the other orbits, which results in different axis scaling. This can be clearly seen in the revised manuscript's Figure 7(c), where the latitude span of the colored points is visibly shorter than that in Figure 7(d).

We sincerely thank the reviewer for this constructive suggestion. We fully agree that the terminology used in the latter section—where the contribution of NEE to XCO₂ enhancements is explicitly analyzed—is clear and precise. However, we would like to clarify that the background determination approach used in the earlier sections (Section 2.3.3) is fundamentally different.

Specifically, in our earlier analysis (e.g., Section 3.1–3.2), the background XCO₂ was derived using a latitude-dependent method combining discrete wavelet transform (DWT) and linear regression. This approach inherently includes the effects of biospheric fluxes such as NEE in the background estimate. As a result, the XCO₂ enhancements derived in that context are interpreted as

primarily due to fossil fuel emissions, with the assumption that NEE contributions are largely accounted for in the background.

In contrast, the analysis in Section 3.3 aims to quantify the influence of NEE on the inversion results. Therefore, we intentionally adopt a different background definition—selecting the minimum value along each orbit—as a conservative estimate that excludes biospheric influences. This allows us to investigate the combined impact of fossil fuel emissions and NEE in a controlled way.

Given this methodological distinction, we believe it is appropriate to use different terminology in each case, to reflect the underlying assumptions and treatment of biospheric fluxes. To improve clarity, we have added explanatory text in the Methods and Results sections to clarify this distinction for the reader.

We hope this resolves the concern, and we sincerely appreciate the reviewer's suggestion to strengthen the presentation.

And Line 598: While the CASA NEE change is small, it seems that CASA is predicting uptake of CO2 by vegetation in winter (a) - Does that make sense? ODIAC predicts an increase in CO2 which makes more sense for a winter-time respiration signal (there is little diel variability in ecosystem respiration so you would expect less NEE diel variability in winter). But I'm surprised that the ODIAC enhancement is so large (>0.5 ppm additional XCO2?)

ANSWER: Thank you very much for your thoughtful comment, which helped us identify an error in our figure preparation. In the originally submitted Figure 9 (now revised as Figure 8), for panel (a), we mistakenly plotted the Model ffXCO₂ as the blue line and the add CASA NEE result as the red line—these were inadvertently swapped. This also explains your question regarding why the CASA NEE appeared to predict net CO₂ uptake in winter, which we agree is not physically reasonable. We have corrected this mistake in the revised manuscript. In fact, for the orbit on this particular day, both CASA and ODIAC NEE simulations predict that vegetation is releasing CO₂ (see Figure 8 a).

Due to residential heating in winter, anthropogenic emissions in Beijing are generally higher during this season. The relatively large wintertime XCO₂ enhancements are therefore primarily driven by increased emissions. However, the relocation of energy-intensive industries outside the city has led to some emission-related concentration increases not being captured within the Beijing administrative boundary. In addition, soil respiration and other biogenic sources are expected to contribute approximately 5% of the total CO₂ emissions during the vegetation dormancy period(Turnbull et al., 2015). These factors may explain why the ODIAC NEE-based enhancements exceed 0.5 ppm in some cases.

Table 1: What is the last column?

ANSWER: In the revised manuscript, we have added a clarification regarding the meaning of the final column in Table 1 to avoid any confusion. This additional explanation ensures that readers can accurately interpret the data presented. "some specific track data inverted using OCO-2 data are bolded, and the average emission scaling factor and a posteriori uncertainty for all tracks in each city are in the last column and highlighted in italics". (Page 28, Line 632-634)

Line 619: "The table below" should be Table 1.

ANSWER: Revised (Page 28, Line 640)

Line 623: "world-class" should probably be "well characterized".

ANSWER: Revised (Page 28, Line 644)

Line 624: Can you clarify if the scaling factor means that the inventories are under or over estimating?

ANSWER: We have added an explanation of the emission scaling factors in the corresponding section. "An emission factor greater than 1 indicates an underestimation by the prior inventory, while a factor less than 1 suggests an overestimation". (Page 28, Line 645-647)

Line 636: That's an interesting point. Do you know why there is a larger transport error in one city vs the other? Would you expect to see a diel variability of CO2 emissions (there is usually a rush hour signal at least) and how would that impact the uncertainties?

ANSWER: We sincerely thank the reviewer for raising this insightful point. In our results, the overall posterior uncertainty among the three cities follows the order Riyadh > Cairo > Beijing. This trend is generally consistent with the notion that emissions from megacities are better characterized. The dominant source of uncertainty differs between Riyadh and Cairo—transport model errors dominate in Riyadh, while observation errors dominate in Cairo. This discrepancy may arise because Cairo has lower overall ffXCO₂ emissions compared to Riyadh, leading to smaller ffXCO₂ enhancements. Compared with simulated ffXCO₂ values, observed local enhancement peaks tend to be sharper and higher, resulting in observation errors that exceed transport model errors in many cases.

For Riyadh, satellite overpasses often pass close to or across emission plumes, making retrievals more susceptible to transport model errors—consistent with findings by Ye et al. (2020) For Los Angeles, the relative contributions of model and measurement errors vary across cases. Among the six orbits analyzed in this study, transport model errors exceed measurement errors in four cases. Compared with Riyadh, the spread in transport model uncertainty over Los Angeles is smaller, possibly due to topographical influences in the Beijing case.

As noted by Ye et al. (2020), transport model uncertainties are closely linked to factors such as total city emissions, the relative location of the plume with respect to the satellite track, transport model performance, and local terrain. Variability in these factors leads to differing temporal patterns in posterior emission uncertainties across orbits.

Line 649: Can you include the actual estimated fluxes alongside the scaling factors?

ANSWER: Revised (Table S3)

Line 668: The "transport" error will be dominated by the higher mixed layer height. The MLH should be included in this discussion.

ANSWER: Revised (Section 4.4)

Line 678: The MLH will be higher in summer days and that may reduce the uncertainties for the footprints.

ANSWER: We fully agree with this point and have accordingly added the following sentence in the

relevant section of the manuscript. (Page 30, Line 702-703)

Line 699: All of these instruments (GeoCARB, TCCON, MicroCARB, etc) are all limited to sunlight times so you can't do day/night inversions. Only DQ-1 can do this type of study.

ANSWER: Revised (Page 32, Line 724-728)

Line 709: VPRM is a parameterized vegetation model. You might want to cite some of the urban configurations such as:

Gourdji, S. M., Karion, A., Lopez-Coto, I., Ghosh, S., Mueller, K. L., Zhou, Y., et al. (2022). A modified Vegetation Photosynthesis and Respiration Model (VPRM) for the eastern USA and Canada, evaluated with comparison to atmospheric observations and other biospheric models. Journal of Geophysical Research: Biogeosciences, 127, e2021JG006290.https://doi.org/10.1029/2021JG006290

Winbourne, J. B., Smith, I. A., Stoynova, H., Kohler, C., Gately, C. K., Logan, B.A., et al. (2022). Quantification of urban forest and grassland carbon fluxes using field measurements and a satellite-based model in Washington DC/Baltimore area. Journal of Geophysical Research: Biogeosciences, 127, e2021JG006568.https://doi.org/10.1029/2021JG006568

Wei, D., Reinmann, A. B., Schiferl, L. D., and Commane, R.: High resolution modeling of vegetation reveals large summertime biogenic CO2 fluxes in New York City, Environmental Research Letters, https://doi.org/10.1088/1748-9326/aca68f, 2022.

ANSWER: added

Line 749: Could you calculate the CO2 fluxes resulting from these scaling factors?

ANSWER: Revised (Table S3)

References

- Alessio, S. M., Alessio, S. M. J. D. s. p., concepts, s. a. f. s., and applications: Discrete wavelet transform (DWT), 645-714, 2016.
- Dai, G., Wu, S., Long, W., Liu, J., Xie, Y., Sun, K., Meng, F., Song, X., Huang, Z., and Chen, W.: Aerosol and cloud data processing and optical property retrieval algorithms for the spaceborne ACDL/DQ-1, Atmos. Meas. Tech., 17, 1879-1890, 10.5194/amt-17-1879-2024, 2024.
- Du, M., Wang, X., Peng, C., Shan, Y., Chen, H., Wang, M., and Zhu, Q.: Quantification and scenario analysis of CO2 emissions from the central heating supply system in China from 2006 to 2025, Applied energy, 225, 869-875, 2018.
- Fan, C., Chen, C., Liu, J., Xie, Y., Li, K., Zhu, X., Zhang, L., Cao, X., Han, G., Huang, Y., Gu, Q., and Chen, W.: Preliminary analysis of global column-averaged CO2 concentration data from the spaceborne aerosol and carbon dioxide detection lidar onboard AEMS, Opt. Express, 32, 21870-21886, 10.1364/OE.517736, 2024.
- Gerbig, C., Körner, S., and Lin, J. C.: Vertical mixing in atmospheric tracer transport models: error characterization and propagation, Atmos. Chem. Phys., 8, 591-602, 10.5194/acp-8-591-2008, 2008.
- Gu, J., Zhang, Y., Yang, N., and Wang, R.: Diurnal variability of the planetary boundary layer height estimated from radiosonde data, Earth and Planetary Physics, 4, 479-492, https://doi.org/10.26464/epp2020042, 2020.
- Gurney, K., Law, R., Rayner, P., and Denning, S.: Transcom 3 experimental protocol, 2000.
- Gurney, K. R., Chen, Y. H., Maki, T., Kawa, S. R., Andrews, A., and Zhu, Z. J. J. o. G. R. A.: Sensitivity of atmospheric CO2 inversions to seasonal and interannual variations in fossil fuel emissions, 110, 2005.
- Han, G., Huang, Y., Shi, T., Zhang, H., Li, S., Zhang, H., Chen, W., Liu, J., and Gong, W.: Quantifying CO2 emissions of power plants with Aerosols and Carbon Dioxide Lidar onboard DQ-1, Remote Sensing of Environment, 313, 114368, https://doi.org/10.1016/j.rse.2024.114368, 2024.
- Lang, M., Guo, H., Odegard, J. E., Burrus, C. S., and Wells Jr, R. O.: Nonlinear processing of a shift-invariant discrete wavelet transform (DWT) for noise reduction, Wavelet Applications II, 640-651.
- Lauvaux, T. and Davis, K. J.: Planetary boundary layer errors in mesoscale inversions of column-integrated CO2 measurements, Journal of Geophysical Research: Atmospheres, 119, 490-508, https://doi.org/10.1002/2013JD020175, 2014.
- Lin, J. C., Gerbig, C., Wofsy, S. C., Andrews, A. E., Daube, B. C., Davis, K. J., and Grainger, C. A.: A near-field tool for simulating the upstream influence of atmospheric observations: The Stochastic Time-Inverted Lagrangian Transport (STILT) model, Journal of Geophysical Research: Atmospheres, 108, https://doi.org/10.1029/2002JD003161, 2003.
- Shekhar, A., Chen, J., Paetzold, J. C., Dietrich, F., Zhao, X., Bhattacharjee, S., Ruisinger, V., and Wofsy, S. C.: Anthropogenic CO2 emissions assessment of Nile Delta using XCO2 and SIF data from OCO-2 satellite, Environmental Research Letters, 15, 095010, 10.1088/1748-9326/ab9cfe, 2020.
- Turnbull, J. C., Sweeney, C., Karion, A., Newberger, T., Lehman, S. J., Tans, P. P., Davis, K. J., Lauvaux, T., Miles, N. L., Richardson, S. J., Cambaliza, M. O., Shepson, P. B., Gurney, K., Patarasuk,

- R., and Razlivanov, I.: Toward quantification and source sector identification of fossil fuel CO2 emissions from an urban area: Results from the INFLUX experiment, Journal of Geophysical Research: Atmospheres, 120, 292-312, https://doi.org/10.1002/2014JD022555, 2015.
- Wu, D., Lin, J. C., Fasoli, B., Oda, T., Ye, X., Lauvaux, T., Yang, E. G., and Kort, E. A.: A Lagrangian approach towards extracting signals of urban CO2 emissions from satellite observations of atmospheric column CO2 (XCO2): X-Stochastic Time-Inverted Lagrangian Transport model ("X-STILT v1"), Geosci. Model Dev., 11, 4843-4871, 10.5194/gmd-11-4843-2018, 2018.
- Yang, Q., Yuan, Q., Yue, L., Li, T., Shen, H., and Zhang, L.: The relationships between PM2. 5 and aerosol optical depth (AOD) in mainland China: About and behind the spatio-temporal variations, Environmental Pollution, 248, 526-535, 2019.
- Ye, X., Lauvaux, T., Kort, E. A., Oda, T., Feng, S., Lin, J. C., Yang, E. G., and Wu, D.: Constraining Fossil Fuel CO2 Emissions From Urban Area Using OCO-2 Observations of Total Column CO2, Journal of Geophysical Research: Atmospheres, 125, e2019JD030528, https://doi.org/10.1029/2019JD030528, 2020.